 Related Commentary, page 1970

mTORC1 is essential for leukemia propagation but not stem cell self-renewal

Takayuki Hoshii,[1] Yuko Tadokoro,[1] Kazuhito Naka,[1] Takako Ooshio,[1] Teruyuki Muraguchi,[1] Naoyuki Sugiyama,[2] Tomoyoshi Soga,[2] Kimi Araki,[3] Ken-ichi Yamamura,[3] and Atsushi Hirao[1]

[1]Division of Molecular Genetics, Cancer and Stem Cell Research Program, Cancer Research Institute, Kanazawa University, Kanazawa, Japan. [2]Institute for Advanced Biosciences, Keio University, Tsuruoka, Japan. [3]Division of Developmental Genetics, Center for Animal Resources and Development, Institute of Resource Development and Analysis, Kumamoto University, Kumamoto, Japan.

Although dysregulation of mTOR complex 1 (mTORC1) promotes leukemogenesis, how mTORC1 affects established leukemia is unclear. We investigated the role of mTORC1 in mouse hematopoiesis using a mouse model of conditional deletion of *Raptor*, an essential component of mTORC1. *Raptor* deficiency impaired granulocyte and B cell development but did not alter survival or proliferation of hematopoietic progenitor cells. In a mouse model of acute myeloid leukemia (AML), *Raptor* deficiency significantly suppressed leukemia progression by causing apoptosis of differentiated, but not undifferentiated, leukemia cells. mTORC1 did not control cell cycle or cell growth in undifferentiated AML cells in vivo. Transplantation of *Raptor*-deficient undifferentiated AML cells in a limiting dilution revealed that mTORC1 is essential for leukemia initiation. Strikingly, a subset of AML cells with undifferentiated phenotypes survived long-term in the absence of mTORC1 activity. We further demonstrated that the reactivation of mTORC1 in those cells restored their leukemia-initiating capacity. Thus, AML cells lacking mTORC1 activity can self-renew as AML stem cells. Our findings provide mechanistic insight into how residual tumor cells circumvent anticancer therapies and drive tumor recurrence.

Introduction

mTOR is an evolutionarily conserved kinase in eukaryotes that plays a critical role in sensing and responding to factors such as nutrient availability, energy sufficiency, stress, hormones, and mitogens. mTOR forms two complexes, designated mTOR complex 1 (mTORC1) and mTORC2. mTORC1, which consists of mTOR, Raptor, and mLST8, phosphorylates multiple substrates, including p70 ribosomal protein S6 kinase (p70S6K) and eukaryote translation initiation factor 4E binding protein 1 (4E-BP1). These target molecules control cell growth (size) and proliferation by modifying protein translation (1). In addition, mTORC1 regulates mitochondrial biogenesis (2, 3) and autophagy (4). mTORC2, formed by mTOR, Rictor, mLST8, SIN1, and Protor, phosphorylates distinct targets including AKT, RAC1, PKCα, and SGK1 (1, 5). Disruption of mTOR and Raptor in mice promotes early embryonic lethality around the implantation stage, whereas deficiency of Rictor, mLST8, or SIN1 causes embryonic lethality at mid-gestation (6, 7). Thus, mTORC1 is indispensable for cell proliferation and survival in early embryogenesis. Although mTORC1 has been assumed to function in growth and metabolism of most cell types, previous studies of mice lacking *Raptor* only in adipocytes or muscle suggest that mTORC1 may have distinct functions in homeostasis depending on the tissue (8, 9). Specifically, *Raptor* deficiency alters mitochondrial biogenesis differently in adipocytes than in muscle. Thus, it is unclear how mTORC1 contributes to the control of growth, proliferation, survival, and differentiation under physiological conditions.

mTORC1 dysregulation promotes leukemogenesis and depletes HSCs (10–14). The tuberous sclerosis complex (TSC) proteins TSC1 and TSC2 negatively regulate mTORC1 signaling. Following phosphorylation by AKT, TSC2 is destabilized, and repression of mTOR signaling is relieved. *Tsc1* deletion in mice causes defects in cell cycling and HSC function due to enhanced mTORC1 activity (10, 11). Deficiency in *Pten*, a negative regulator of PI3K/AKT signaling, also impairs the quiescence of HSCs, leading to their depletion. *Pten* deficiency in hematopoietic cells promotes myeloproliferative disease followed by development of leukemia (12, 14, 15). Since these phenotypes are inhibited by the mTORC1 inhibitor rapamycin, mTORC1 activation has been thought to induce HSC depletion and leukemogenesis. Currently, however, it is unclear how altered mTORC1 affects the behavior of established leukemia.

Recent improvements in cell purification and transplantation techniques have enabled identification of tumor cells capable of initiating and propagating malignancy, known as cancer stem cells (CSCs). Previous studies have suggested that common mechanisms regulate stem cell properties (stemness) in both HSCs and leukemia stem cells (CSCs in leukemia), leading to the idea that leukemia stem cells may originate from HSCs (16). On the other hand, it has been reported that introduction of oncogene fusion constructs that promote acute myeloid leukemia (AML), such as the *MLL-ENL*, *MLL-AF9*, and *MOZ-TIF2* genes, into committed myeloid progenitors transforms the cells and promotes the acquisition of self-renewal ability (17–21). A recent study using a large number of primary human AML patient samples indicated that human AML stem cells are immunophenotypically similar to progenitors, including lymphoid-primed multipotential progenitors and granulocyte-macrophage progenitors (GMPs), rather than to HSCs (22). Furthermore, the gene expression profiles AML stem cells is similar to that of committed myeloid progenitors, suggesting that AML stem cells may be derived from myeloid progenitors. In addition, it has been reported that the expression pattern of genes that are associated with stem cell phenotypes in AML is similar to that in HSCs or embryonic stem cells (18, 22, 23). These find-

Conflict of interest: The authors have declared that no conflict of interest exists.
Citation for this article: *J Clin Invest.* 2012;122(6):2114–2129. doi:10.1172/JCI62279.

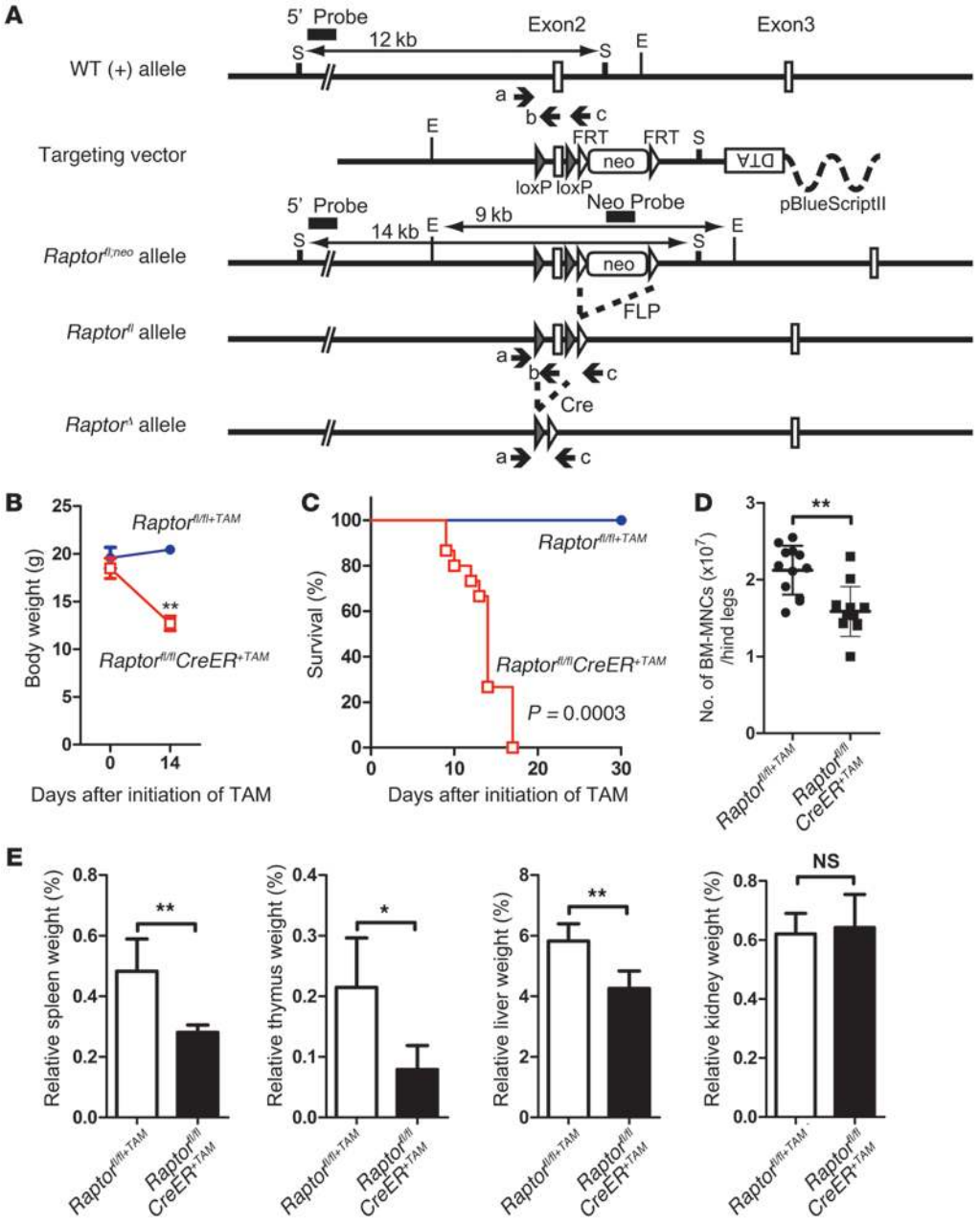

Figure 1

Conditional deletion of *Raptor* causes abnormalities in the hematopoietic organs of adult mice. (**A**) Targeting strategy to create the floxed *Raptor* (*Raptor*^{fl}) allele. The targeting vector includes a FRT-flanked neo cassette (PGK promoter–driven neomycin resistance gene) for positive selection and a diphtheria toxin A (DTA) gene for negative selection. *Raptor* exon 2 is flanked by loxP sites. The neo cassette of the *Raptor*$^{fl;neo}$ allele was removed by crossing *Raptor*$^{fl;neo}$ mice with *CAG-FLP* mice. Exon 2 was removed by Cre recombinase to give the *Raptor*$^{\Delta}$ allele. Probes for Southern blotting (5′ probe, Neo) and primers for PCR (a, b, c) are indicated. E, *Eco*RI; S, *Sac*I. (**B**) Body weight of *Raptor*$^{fl/fl+TAM}$ (control) and *Raptor*$^{fl/fl}$*CreER*$^{+TAM}$ (*Raptor*-deficient) mice. Data shown are the mean body weight ± SD ($n = 5$). (**C**) Survival of control and *Raptor*-deficient mice. $P = 0.0003$ (log-rank test; $n = 15$). (**D**) Decreased numbers of BM-MNCs. Data shown are the mean BM-MNC number ± SD in hind legs of control and *Raptor*-deficient mice at 10 days post-TAM ($n = 12$). (**E**) Organ weights of control and *Raptor*-deficient mice at 10 days post-TAM. Data shown are the mean relative organ weight (% of total body weight) ± SD ($n = 5$). *$P < 0.05$, **$P < 0.01$ (Student's *t* test).

ings suggest that AML stem cells originate from myeloid progenitors that have acquired stemness properties during leukemogenesis. Thus, determining how mTORC1 functions in both hematopoiesis and leukemia could provide novel insights into the mechanisms controlling the properties of CSCs.

Rapamycin and its derivatives are allosteric inhibitors of mTORC1 and likely inhibit its function through direct interaction. However, 4E-BP1, a direct target of mTORC1, is reportedly a rapamycin-insensitive substrate (24, 25). Two recent phosphoproteomic analyses revealed that there are critical differences between

rapamycin and ATP-competitive mTOR inhibitors (26, 27). Thus, genetic approaches will be likely be the most effective for inactivation of mTORC1 in vivo, because the regulation of mTORC1 by chemical inhibitors is complicated and may not produce predictable reductions in mTORC1 activity.

In this study, we generated mice with an inducible conditional deletion of *Raptor*, which encodes an essential component of mTORC1, and investigated the physiological and pathological roles of mTORC1 in normal and malignant hematopoiesis. These studies show striking evidence that the self-renewal and tumor-initiating properties of leukemia stem cells are differentially dependent on mTORC1.

Results

Conditional deletion of Raptor causes abnormalities in hematopoietic organs of adult mice. To investigate mTORC1 function in normal hematopoiesis in vivo, we used a tamoxifen-inducible (TAM-inducible) CreER system to generate mutant mice in which *Raptor* could be depleted in all tissues by i.p. injection of TAM (Figure 1A and Supplemental Figure 1, A and B; supplemental material available online with this article; doi:10.1172/JCI62279DS1). These *Raptor$^{fl/fl}$;Rosa-CreER^{T2}* mice are referred to herein as *Raptor$^{fl/fl}$CreER* mice before TAM administration and as *Raptor$^{fl/fl}$CreER^{+TAM}* mice after TAM administration and *Raptor* deletion. The corresponding control mice, in which *Raptor* is not deleted, are referred to as *Raptor$^{fl/fl+TAM}$* or *Raptor$^{fl/+}$CreER^{+TAM}* mice. As expected, embryonic fibroblasts derived from *Raptor$^{fl/fl}$CreER*, but not from *Raptor$^{fl/+}$CreER*, mice showed loss of Raptor protein, resulting in dramatic inhibition of proliferation after TAM treatment (Supplemental Figure 1C). We also detected a remarkable reduction in p-S6 and p–4E-BP1 with Western blotting and by flow cytometry (Supplemental Figure 1, D and E), confirming that we had successfully established a system for the conditional inactivation of mTORC1. After administration of TAM, *Raptor$^{fl/fl}$CreER^{+TAM}* mice rapidly lost body weight and died within 17 days, likely due to severe intestinal dysfunction, because we found dramatic loss of villi associated with increased apoptosis in the epithelial layer (Figure 1, B and C, and Supplemental Figure 1, F–I). At 10 days after the last TAM treatment (post-TAM), we found that the number of wbc in peripheral blood (PB), as well as mononuclear cells (MNCs) in BM, was significantly decreased in the absence of *Raptor* (Figure 1D and Supplemental Figure 2A). The masses of the thymus, spleen, and liver were also reduced in *Raptor$^{fl/fl}$CreER^{+TAM}* mice compared with *Raptor$^{fl/fl+TAM}$* mice (Figure 1E). These abnormalities were not observed in *Raptor$^{fl/+}$CreER^{+TAM}* mice (Supplemental Figure 3, A and B), confirming that the phenotypes are caused by *Raptor* deletion and not by nonspecific effects of Cre expression.

Deletion of Raptor impairs granulocyte and B cell development but does not alter progenitor cell survival or proliferation. To examine which cell populations are affected by *Raptor* deletion, we analyzed BM-MNCs by flow cytometry with Abs to several cell surface markers. In particular, *Raptor* deficiency resulted in decreased numbers of Mac-1$^+$Gr-1$^+$ granulocytes, although the number of Mac-1$^+$Gr-1$^-$ myeloid lineage cells increased in BM (Figure 2A and Supplemental Figure 2, B, G, and H). *Raptor* deficiency led to dramatic decreases in B220^{lo}IgM$^-$ cells (early B cell precursors: pro/pre-B cells) and B220^{lo}IgM$^+$ cells (immature B cells), but not B220^{hi}IgM$^+$ cells (mature B cells) (Figure 2A and Supplemental Figure 2, I and J). These abnormalities were not observed in *Raptor$^{fl/+}$CreER^{+TAM}* mice (Supplemental Figure 3C). In contrast to its effects on differentiated cells, *Raptor* deficiency was much less detrimental to hematopoietic progenitor cells. In the absence of *Raptor*, the number of common lymphoid progenitors (CLPs) was normal, and the number of GMPs was significantly increased (Figure 2A and Supplemental Figure 2, C–F). Importantly, the loss of differentiated cells in *Raptor$^{fl/fl}$CreER^{+TAM}* mice appeared to be due to increased apoptosis in these populations (Lin$^+$ cells and Mac-1$^+$Gr-1$^+$cells), since *Raptor*-deficient c-Kit$^+$Sca-1$^-$Lin$^-$ (K$^+$S$^-$L$^-$) cells, including common myeloid progenitors (CMPs) and GMPs, did not show any obvious changes in apoptosis (Figure 2B). Cell cycle status as determined by in vivo BrdU incorporation was not altered by *Raptor* deficiency in any cell population examined (Figure 2C).

To evaluate the effect of *Raptor* deficiency on the colony-forming ability of myeloid cells in vitro, we isolated c-Kit$^+$Sca-1$^+$Lin$^-$ (K$^+$S$^+$L$^-$) cells, which include HSCs and multipotent progenitors (MPPs), or GMPs from the BM of *Raptor$^{fl/fl}$CreER^{+TAM}* mice and cultured them in semisolid medium. Loss of Raptor dramatically inhibited formation of colonies with high proliferative potential in K$^+$S$^+$L$^-$ cells (Figure 2D and Supplemental Figure 4A). Retroviral transduction of human *RAPTOR* (*hRAPTOR*) rescued the defective colony-forming ability of *Raptor*-deficient K$^+$S$^+$L$^-$ cells (Supplemental Figure 4, B and C). In contrast, GMPs with and without *Raptor* showed comparable colony-forming abilities in this assay (Figure 2E and Supplemental Figure 4A). These data suggest that mTORC1 activity is not needed for the proliferation or differentiation of GMPs, but it may be essential for these processes in the more immature progenitor cells. To evaluate the activity of *Raptor*-deficient progenitor cells under more physiological conditions, we cultured K$^+$S$^+$L$^-$ cells on a layer of OP9 stromal cells. Whereas both B220$^+$ B cells and Mac-1$^+$ myeloid cells were generated from control K$^+$S$^+$L$^-$ cells under these culture conditions, *Raptor* deficiency strikingly decreased the number of B220$^+$ cells while increasing the number of Mac-1$^+$ cells (Figure 2F). In this culture condition, the emerging B cells are produced through *Raptor*-deficient B cell precursors; the defect in B cell precursors therefore resulted in decreased B cell production. Thus, these data are consistent with our in vivo observations (Figure 2A). To exclude the possibility that Raptor is needed for the microenvironment supporting hematopoiesis in vivo, we transplanted *Raptor$^{fl/fl}$CreER* BM-MNCs (CD45.2) plus the same number of competitor WT BM-MNCs (CD45.1/CD45.2) into recipient mice (CD45.1). At 2 weeks post-TAM, increased GMP and decreased granulocyte levels were present among *Raptor$^{fl/fl}$CreER^{+TAM}* BM-MNCs (Supplemental Figure 5, A and B), also consistent with the flow cytometry data shown in Figure 2A. These findings indicate that the effects of *Raptor* deficiency on myeloid lineage cells are cell intrinsic and demonstrate that Raptor is not essential for the survival or proliferation of myeloid progenitor cells.

Raptor loss has differential effects on phosphorylation of mTORC1 effectors in different hematopoietic cell contexts. To investigate the effects of *Raptor* deficiency on mTORC1 signaling, we quantitatively evaluated the phosphorylation status of mTORC1 effectors by flow cytometric analysis using intracellular staining with an anti–p-S6 (S235/236) or anti–p-4E-BP1 (T36/45) Ab (Figure 3A), as we had done with embryonic fibroblasts (Supplemental Figure 1E). In control mice, the HSC/MPP (K$^+$S$^+$L$^-$) population contained both p-S6^{lo}p–4E-BP1^{lo} (HSC) and p-S6^{hi}p–4E-BP1^{hi} (MPP) cells. Control CMP and GMP populations mainly consisted of p-S6^{hi}p–4E-BP1^{hi} cells, whereas the majority of control B220$^+$ cells were p-S6$^{lo/neg}$p–4E-BP1$^{lo/neg}$, with a minority of p-S6^{hi}p–4E-BP1^{hi} cells. As expected, *Raptor* deficiency in vivo markedly decreased 4E-BP1 phosphory-

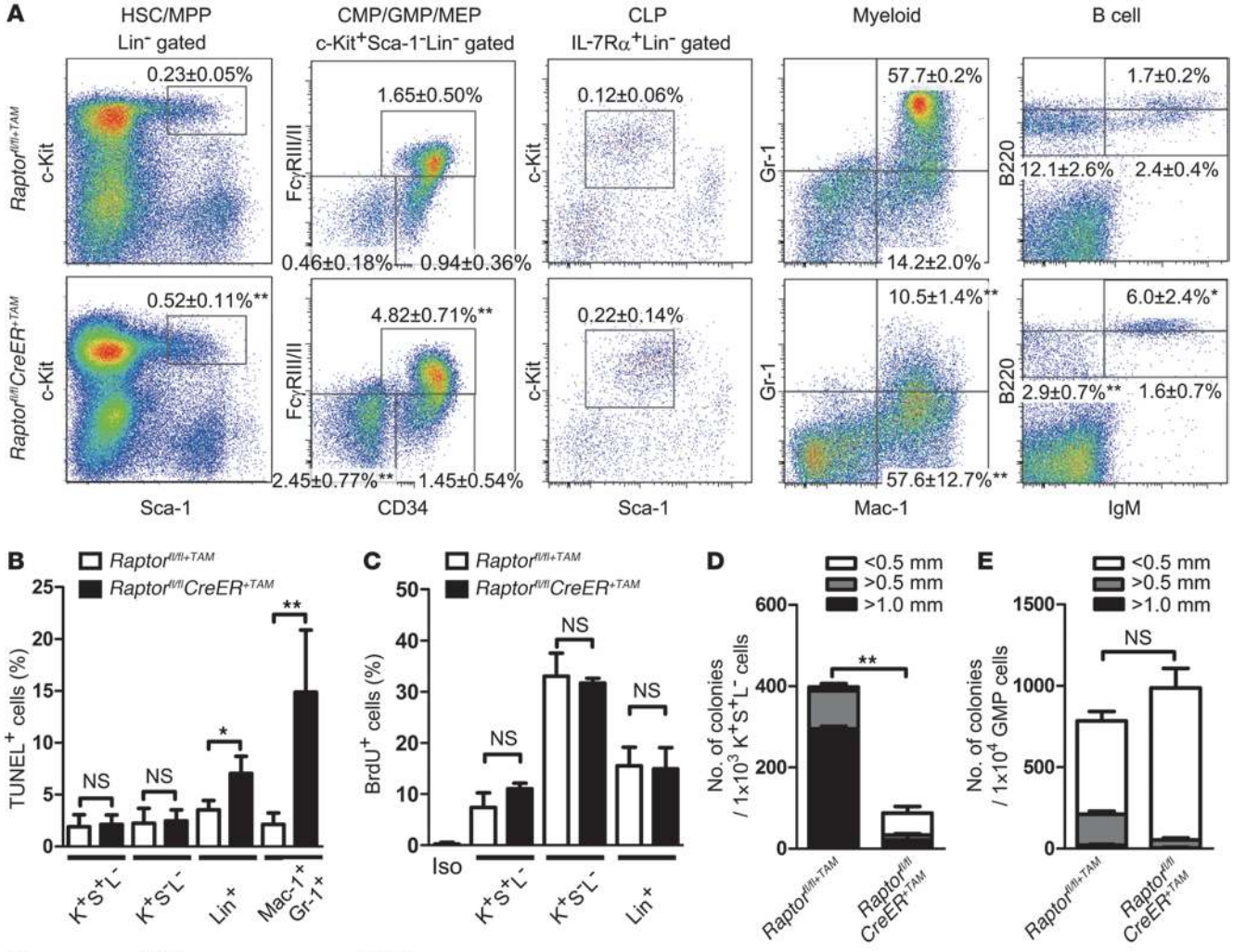

Figure 2

Deletion of *Raptor* impairs granulocyte and B cell development but does not alter progenitor cell survival or proliferation. (**A**) Flow cytometric analysis of BM-MNCs from control and *Raptor*-deficient mice. Images represent data for HSCs/MPPs ($K^+S^+L^-$), CMPs ($Lin^-c\text{-}Kit^+Sca\text{-}1^-FcgRIII/II^-CD34^+$), GMPs ($Lin^-c\text{-}Kit^+Sca\text{-}1^-FcgRIII/II^+CD34^+$), MEPs ($Lin\text{-}c\text{-}Kit^+Sca\text{-}1^-FcgRIII/II^-CD34^-$), CLPs ($IL\text{-}7R\alpha^+Lin\text{-}c\text{-}Kit^{mid}Sca\text{-}1^{mid}$), myeloid lineage cells (Mac-1/Gr-1), and B lineage cells (B220/IgM). Values are the mean percentage ± SD of the specified subpopulation among total BM-MNCs ($n = 4$). (**B**) Apoptosis. BM-MNCs from control and *Raptor*-deficient mice were subjected to TUNEL staining, and the indicated subpopulations were analyzed by flow cytometry. Data shown are the mean ± SD of $TUNEL^+$ cells ($n = 3$). (**C**) Cell cycle. BrdU was injected i.p. into mice 2 hours prior to sacrifice. The indicated BM cell populations were stained with an anti-BrdU Ab and analyzed by flow cytometry. Data are the mean percentage ± SD of $BrdU^+$ cells ($n = 3$). (**D** and **E**) Colony-forming ability. $K^+S^+L^-$ cells (**D**) and GMP cells (**E**) were isolated from BM-MNCs of control and *Raptor*-deficient mice and cultured for 10 days in semisolid medium. Data are the mean colony number ± SD ($n = 3$). Colony diameters are indicated. (**F**) Flow cytometric analysis of the differentiation into myeloid and B lineage cells of control and *Raptor*-deficient $K^+S^+L^-$ cells cultured on stromal cells. *Raptor*$^{fl/fl}$ or *Raptor*$^{fl/fl}$*CreER* $K^+S^+L^-$ cells were cultured on a layer of OP-9 stromal cells for 2 weeks in the presence or absence of TAM. Data shown are the percentage ± SD of $B220^+$ $Mac\text{-}1^+$ cells among $CD45^+$-gated cells ($n = 3$). One flow cytometric analysis representative of 3 independent experiments is shown. $^*P < 0.05$, $^{**}P < 0.01$ (Student's *t* test).

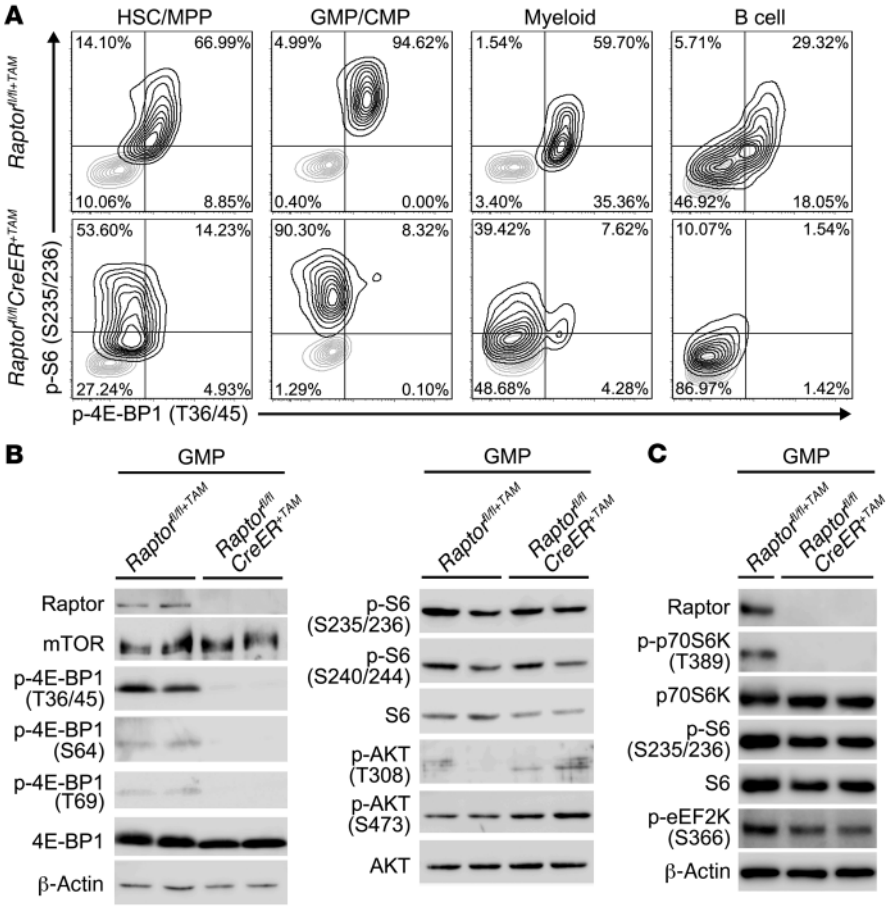

Figure 3
Deletion of *Raptor* has differential effects on phosphorylation of mTORC1 effectors in different hematopoietic cell contexts. (**A**) Flow cytometric analysis of intracellular p-S6 and p–4E-BP1. Data shown are levels of p-S6 (S235/236) and p–4E-BP1 (T36/45) in the indicated BM MNC subpopulations from control and *Raptor*-deficient mice. Cells were collected 10 days after the last injection of TAM. (**B**) Phosphorylation of mTOR signaling pathway proteins in GMPs. Lysates of GMPs isolated from control and *Raptor*-deficient mice were immunoblotted to detect the indicated proteins. β-Actin was used as loading control. Results are representative of at least 3 independent trials. (**C**) Phosphorylation of p70S6K and its substrates in GMPs. Lysates of GMPs isolated from control and *Raptor*-deficient mice were immunoblotted to detect the indicated proteins. β-Actin was used as loading control. Results are representative of at least 3 independent trials.

lation in all hematopoietic cell populations. Unexpectedly, however, S6 phosphorylation was not inhibited in GMPs and CMPs. In contrast, S6 phosphorylation was markedly downregulated in *Raptor*-deficient B220$^+$ B cells.

To confirm these findings biochemically, we performed immunoblotting analyses of GMPs. Consistent with our flow cytometric analyses, phosphorylation of S6 (at S235/236 and S240/244) was not altered by *Raptor* deficiency (Figure 3B). In contrast, 4E-BP1 phosphorylation at all 4 sites, T36/45, S64, and T69, was strongly inhibited in the absence of Raptor. The phosphorylation of p70S6K, a direct target of mTORC1, was also dramatically inhibited by Raptor deficiency, whereas phosphorylation of eEF2K, a target molecule of p70S6K, was not affected in GMPs (Figure 3C), suggesting that S6 and eEF2K are phosphorylated in an mTOR-independent manner, as previously reported (28–30). Thus, these results indicate that the phosphorylation of downstream molecules in the mTORC1 pathway is highly variable among hematopoietic lineages.

Raptor deficiency suppresses AML progression in vivo. To evaluate the role of mTORC1 in established AML, we investigated the effects of mTORC1 inactivation via genetic ablation of *Raptor* in a murine AML model. To create a representative AML model, we first inserted the *MLL-AF9* fusion gene (17, 18, 21) into K$^+$S$^+$L$^-$ cells isolated from *Raptor*$^{fl/fl}$, *Raptor*$^{+/+}$*CreER*, or *Raptor*$^{fl/fl}$*CreER* mice by using retrovirus-mediated transfer. We then transplanted these genetically modified cells into lethally irradiated syngeneic recipients to generate *Raptor*$^{fl/fl}$, *Raptor*$^{+/+}$*CreER*, and *Raptor*$^{fl/fl}$*CreER* AML mice, respectively (Figure 4A). In the absence of TAM treatment, all 3 sets of recipient mice soon developed AML characterized by a significant increase in GFP$^+$Mac-1$^+$ leukemic cells in spleen and BM (Supplemental Figure 6). To determine the effect of mTORC1 inactivation on AML in vivo, we carried out a second transplantation in which BM-MNCs from AML mice were transferred into fresh recipients (along with WT rescue cells). We administered TAM to these animals to delete *Raptor* and monitored their survival and AML progression. TAM injection significantly prolonged the survival of the *Raptor*$^{fl/fl}$*CreER* AML mice, but not that of *Raptor*$^{fl/fl}$ AML mice (Figure 4, B and C) or *Raptor*$^{+/+}$*CreER* AML mice (Supplemental Figure 7). These data indicate that the prolonged life span of the *Raptor*$^{fl/fl}$*CreER* AML mice treated with TAM was due to *Raptor* deficiency and not Cre toxicity (Supplemental Figure 7A).

Although all *Raptor*$^{fl/fl}$*CreER*$^{+TAM}$ (*Raptor*-deficient) AML mice died by 42 days post-TAM, the reason for the deaths was the progression of AML cells with incomplete deletion of the *Raptor* gene. Therefore, we analyzed the characteristics of the AML cells at 14 days post-TAM, because we found efficient deletion of the *Raptor* gene in all *Raptor*$^{fl/fl}$*CreER*$^{+TAM}$ AML mice at this time point. Consistent with their prolonged survival, the number of wbc in the PB of *Raptor*$^{fl/fl}$*CreER*$^{+TAM}$ AML mice at 14 days post-TAM injection decreased dramatically compared with that in control *Raptor*$^{fl/fl}$ *CreER*$^{-TAM}$ AML mice (Figure 4D). Previous reports on this AML model have indicated that c-Kit marks undifferentiated AML cells (17, 18, 31). In the PB of our control AML mice, most AML cells (GFP$^+$) did not express c-Kit (Figure 4E), indicating that AML cells

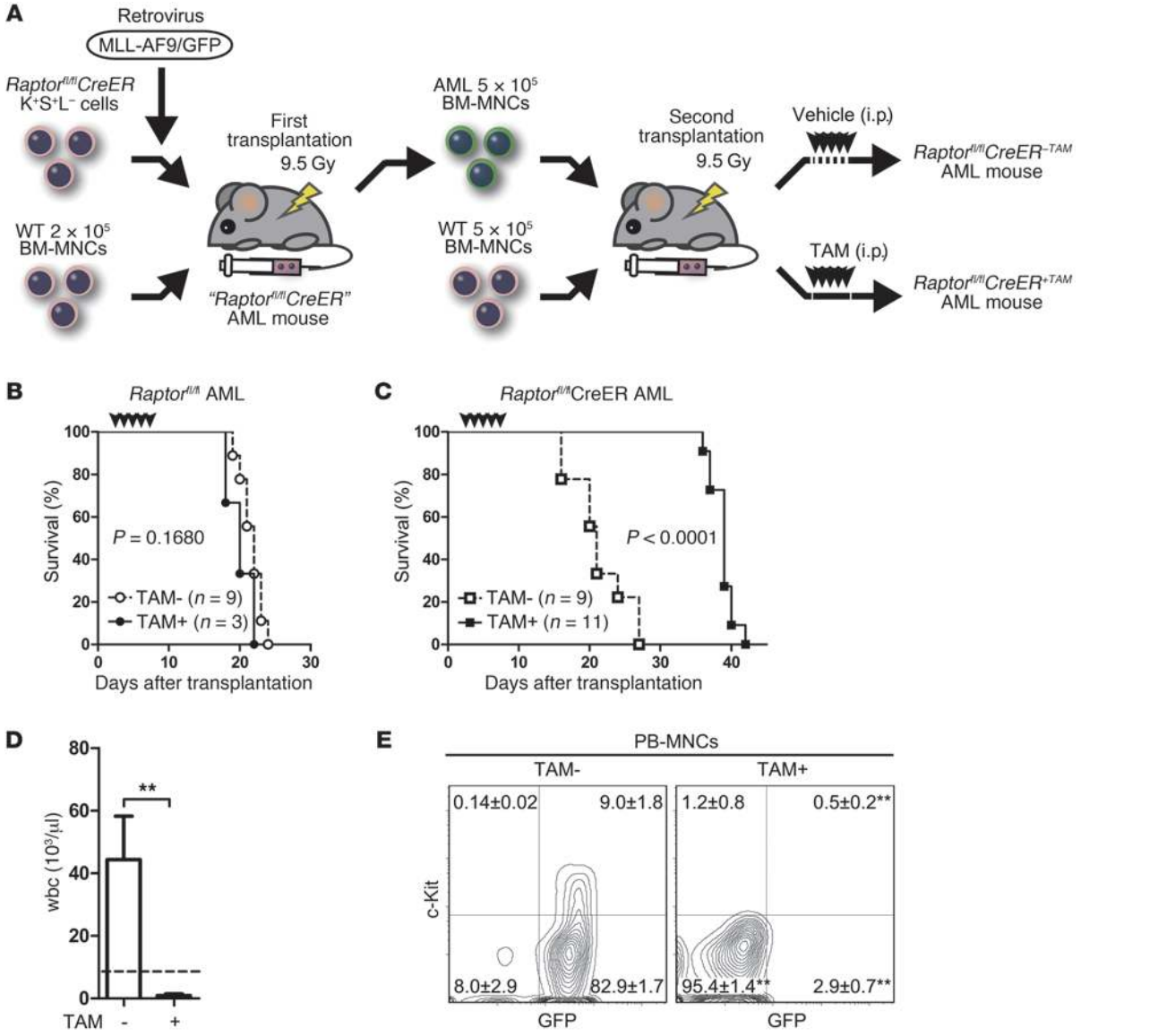

Figure 4

Generation of a *Raptor*-deficient murine AML model. (**A**) Experimental design for a *Raptor*-deficient murine AML model. (**B** and **C**) Survival of AML mice. *Raptor*$^{fl/fl}$ AML mice (**B**) and *Raptor*$^{fl/fl}$*CreER* AML mice (**C**) were established as illustrated in **A**. BM-MNCs from these animals were transplanted into a fresh set of recipients (along with rescue cells), and these animals were treated with oil diluent as the control (TAM–) or with TAM (TAM+) to generate the indicated control and *Raptor*-deficient AML mice. *P* value were determined by the log-rank test. (**D**) Number of wbc in PB. PB samples were obtained from the *Raptor*$^{fl/fl}$*CreER* AML mice at 14 days after control or TAM treatment. Data shown are mean number ± SD (TAM–, $n = 6$; TAM+ $n = 9$). The horizontal dotted line is the mean value of the number of wbc in normal adult mice (8 weeks old, $n = 5$). (**E**) Flow cytometric analyses of AML cells in PB. PB samples were obtained from the *Raptor*$^{fl/fl}$*CreER* AML mice at 14 days after control or TAM treatment. Representative data are shown for GFP/c-Kit expression in PB-MNCs. Values in panels are the mean percentage ± SD for the indicated subpopulations ($n = 4$). $^{**}P < 0.01$ (Student's *t* test).

present in the circulation had differentiated. Upon TAM injection, AML cells disappeared from the PB of *Raptor*$^{fl/fl}$*CreER*$^{+TAM}$ AML mice (Figure 4E), but not of *Raptor*$^{+/+}$*CreER*$^{+TAM}$ AML mice (Supplemental Figure 7B). Pharmaceutical inhibition of mTORC1 by rapamycin slightly prolonged the survival of AML mice, but it had a milder effect than *Raptor* deficiency (Supplemental Figure 8, A and B). Thus, *Raptor* deficiency significantly suppressed AML progression in vivo, thereby prolonging the life span of AML mice.

mTORC1 inactivation induces dramatic levels of apoptosis in differentiated, but not undifferentiated, AML cells. Next, we investigated the effect of *Raptor* deficiency on AML cells in BM. Interestingly, the reduction in the number of AML cells in the BM of *Raptor*$^{fl/fl}$ *CreER*$^{+TAM}$ AML mice was much milder than that observed in the PB of the same animals (Figure 5, A and C). In addition, platelet counts were not restored to normal in mutant AML mice (Figure 5B). These data suggest that *Raptor* deficiency did not rescue the

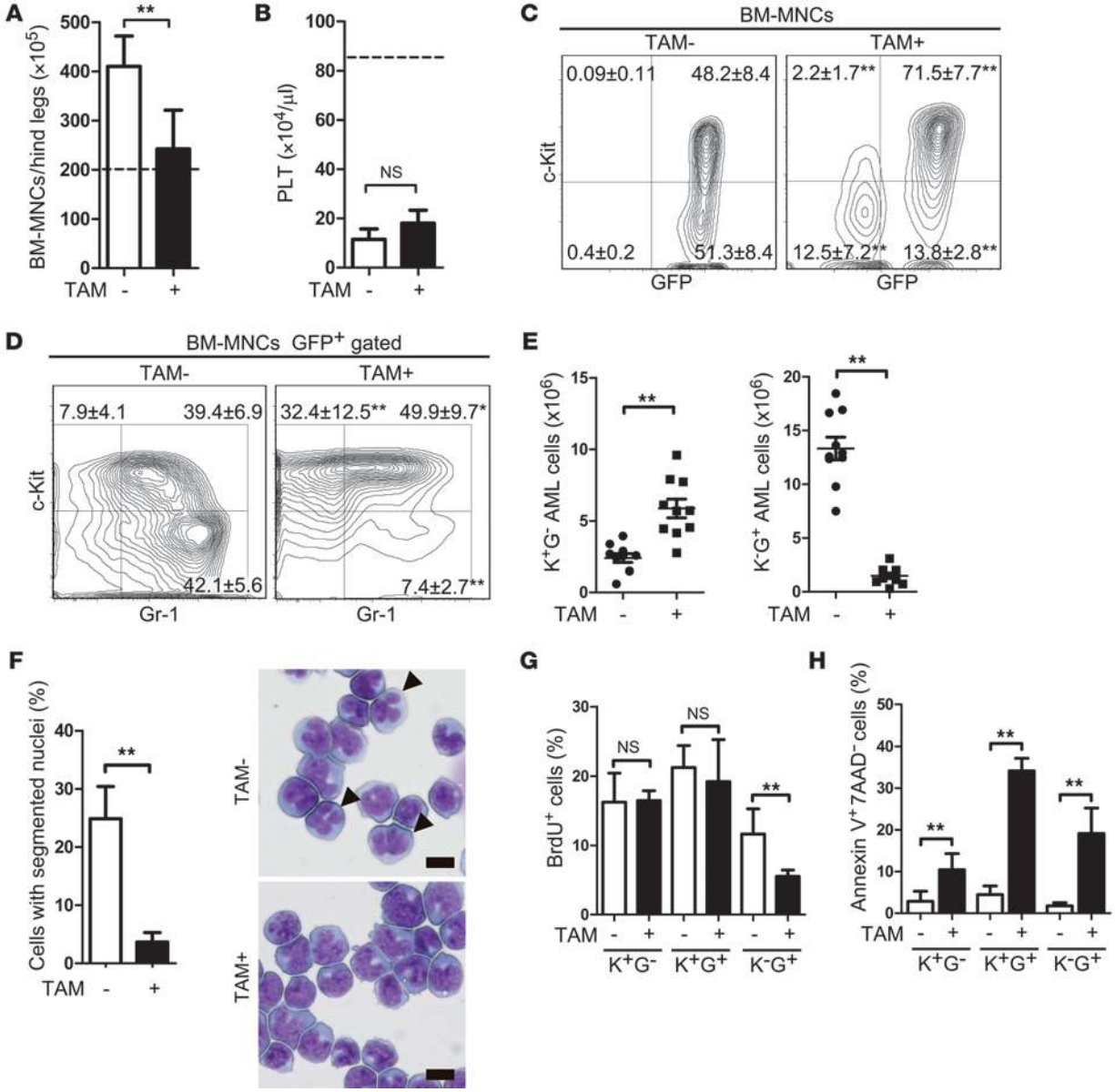

Figure 5

Undifferentiated AML cells are resistant to loss of mTORC1 activity. The *Raptor*$^{fl/fl}$*CreER* AML mice were analyzed 14 days after control or TAM treatment. (**A** and **B**) Number of BM-MNCs in BM (**A**: TAM–, $n = 6$; TAM+, $n = 5$) and of platelets (PLT) in PB (**B**: TAM–, $n = 6$; TAM+, $n = 9$). Data are mean number ± SD of the indicated hematopoietic cell type. Horizontal dotted lines are mean values of the indicated hematopoietic parameters in normal adult mice (8 weeks old, $n = 5$). (**C** and **D**) Flow cytometric analyses of AML cells in BM. Representative data are shown for GFP/c-Kit expression in BM-MNCs (**C**) and for c-Kit/Gr-1 expression in GFP$^+$-gated BM-MNCs (**D**). Values are the mean percentage ± SD for the indicated subpopulations (**C**, $n = 10$; **D**, $n = 3$). (**E**) Absolute numbers of K$^+$G$^-$ and K$^-$G$^+$ cells in the hind legs of the *Raptor*$^{fl/fl}$*CreER* AML mice (TAM– or TAM+). Data shown are the values for individual mice ($n = 10$ per group). Horizontal lines are mean values. (**F**) Morphological analysis of AML cells. GFP$^+$ cells from the BM of AML mice were stained with May-Grünwald/Giemsa. Data are the mean percentage ± SD of AML cells containing segmented nuclei ($n = 5$). Right panels show representative images of GFP$^+$ cells. Scale bars: 10 μm. Arrowheads indicate AML cells with segmented nuclei (differentiated AML cells). (**G**) Cell cycle. BrdU was injected i.p. into AML mice 2 hours prior to sacrifice. AML cells were harvested, stained with an anti-BrdU Ab, and analyzed by flow cytometry. Data are the mean percentage ± SD of BrdU$^+$ cells in the indicated AML cell subpopulations ($n = 5$). (**H**) Apoptosis. Data shown are the mean percentage ± SD of Annexin V$^+$7AAD$^-$ cells in the indicated AML cell subpopulations ($n = 5$). $^*P < 0.05$, $^{**}P < 0.01$ (Student's *t* test).

hematopoietic failure seen in AML mice due to the occupation of the BM by AML cells.

To evaluate the properties of AML cells in the BM of *Raptor*$^{fl/fl}$ *CreER*$^{+TAM}$ AML mice, we analyzed expression of cell surface markers at various stages of AML cell differentiation. Previous reports on this AML model have shown that AML stem cells are highly enriched in the c-Kit$^+$Gr-1$^-$ (K$^+$G$^-$) population (31). Upon TAM injection, c-Kit$^+$ AML cells were enriched in the BM of *Raptor*$^{fl/fl}$

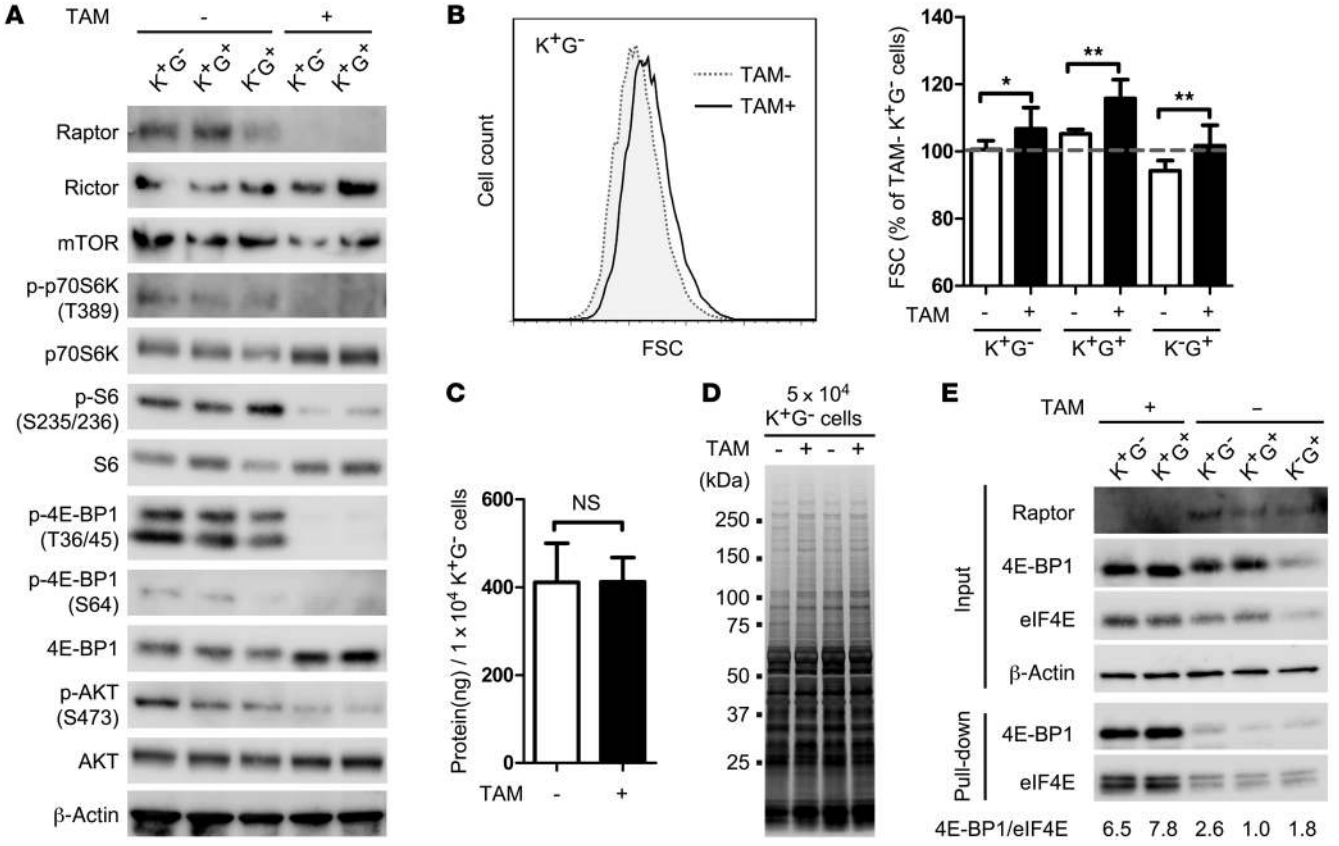

Figure 6

4E-BP1–independent cell growth of *Raptor*-deficient AML cells. (**A**) Phosphorylation of mTOR signaling pathway proteins. Lysates were prepared from the indicated AML cell subpopulations and immunoblotted to detect the indicated proteins. (**B**) Flow cytometric analysis of cell size. Left: Representative histogram shows forward scatter (FSC) of K^+G^- AML cells from the mice in **A**. Right: Quantification. All FSC values were normalized to the mean value (dotted line) obtained for K^+G^- AML cells from control AML mice in 10 independent experiments. Data shown are mean normalized FSC values ± SD (n = 10). (**C** and **D**) Amount of protein in K^+G^- AML cells. Lysates were prepared from K^+G^- AML cells 14 days post-TAM. Proteins were quantified with a BCA protein assay (**C**), and SDS-PAGE was performed, followed by silver staining, to visualize protein levels (**D**). Data in **C** are the mean ± SD of the amount of protein (ng) in 1 × 10^4 K^+G^- AML cells (n = 8). (**E**) 7-methyl GTP pull-down assay. Lysates were prepared from the indicated AML cell subpopulations, incubated with 7-methyl GTP-Sepharose beads, washed, and immunoblotted to detect the indicated proteins. Numbers below the panel are the ratios of the intensity of the 4E-BP1 and eIF4E protein band signals. *P < 0.05, **P < 0.01 (Student's t test).

CreER AML mice (Figure 5C), but not *Raptor*$^{+/+}$*CreER* AML mice (Supplemental Figure 7, D and E). In addition, *Raptor* deficiency increased the proportion of K^+G^- cells, whereas the proportion of K^-G^+ cells decreased (Figure 5D). The absolute number of K^-G^+ AML cells dropped precipitously upon deletion of *Raptor*, whereas that of K^+G^- AML cells increased (Figure 5E). Morphological analysis of AML cells confirmed that *Raptor* deficiency was associated with decreased differentiation, as judged by the lack of cells with segmented nuclei (Figure 5F). These data suggest that differentiated AML cells, but not undifferentiated AML cells, require mTORC1 for survival or proliferation. In vivo BrdU incorporation studies showed that loss of *Raptor* resulted in a decrease in proliferation of K^-G^+ AML cells, but it had no effect on either K^+G^+ or K^+G^- AML cells (Figure 5G). In contrast, apoptosis was increased by *Raptor* deficiency in all AML cell populations examined but was most highly elevated in K^+G^+ AML cells (Figure 5H). No significant effect on apoptosis was seen in these cell populations from control *Raptor*$^{+/+}$*CreER* AML mice (Supplemental Figure 7F). These data indicate that the loss of differentiated AML cells following mTORC1 inactivation is due to both increased apoptosis and decreased cell proliferation, whereas undifferentiated (K^+G^-) AML cells are enriched because of reduced apoptosis.

4E-BP1–independent cell growth of AML cells. To examine the molecular changes occurring in AML cells lacking mTORC1 activity, we carried out immunoblotting analyses. The phosphorylation of p70S6K, 4E-BP1, and S6 was dramatically suppressed in *Raptor*-deficient, but not control, AML cells, including the AML stem cell population (K^+G^- cells), indicating downregulated mTORC1 activity (Figure 6A and Supplemental Figure 7G). Rapamycin treatment effectively suppressed the phosphorylation of p70S6K and S6 in AML cells, whereas it did not affect phosphorylation of 4E-BP1 (Supplemental Figure 8C). A similar phenomenon was observed in embryonic fibroblasts (Supplemental Figure 1E), which is consistent with previous reports showing that 4E-BP1 is a rapamycin-insensitive mTORC1 target (24, 25). Although it has been reported that mTORC1 inactivation leads to enhanced AKT phosphorylation in some cell types

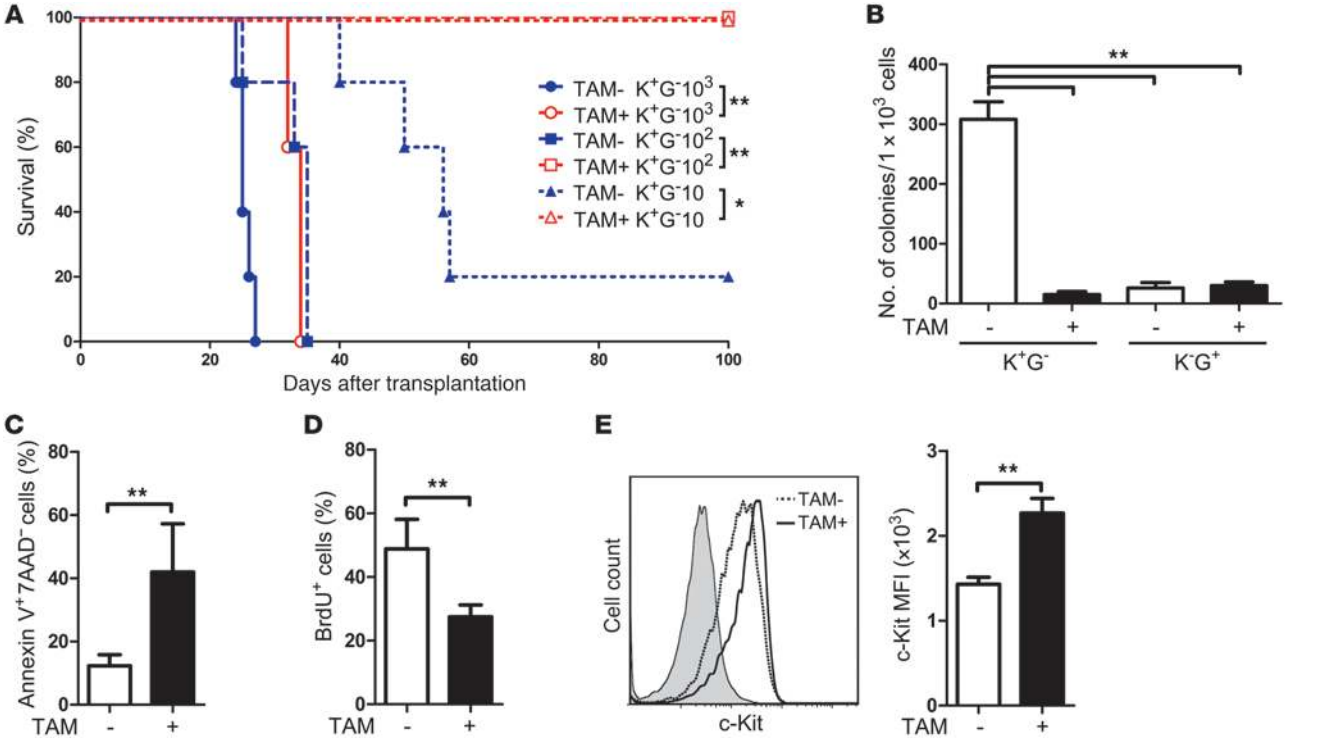

Figure 7

Raptor-deficient AML stem cells show defective leukemia-initiating capacity. (**A**) Limiting dilution transplantation assay. The indicated numbers of K^+G^- AML cells from the mice 14 days after control or TAM treatment were transplanted into lethally irradiated recipients along with WT BM-MNCs (rescue cells), and survival was monitored (n = 5/group). *P < 0.05, **P < 0.01 (log-rank test). (**B**) Colony-forming ability of AML cells. K^-G^+ and K^+G^- AML cells were isolated from *Raptor*$^{fl/fl}$*CreER* AML mice 14 days after control or TAM treatment and cultured in semisolid medium for 7 days. Data are the mean colony numbers ± SD (n = 3). (**C**) Apoptosis of K^+G^- AML cells after 12 hours of stimulation with the cytokines SCF, IL-3, and IL-6. Data shown are the mean percentage ± SD of Annexin V^+7AAD^- cells (n = 8). (**D**) Cell cycle of K^+G^- AML cells after 12 hours of stimulation with the same set of cytokines. Data shown are the mean percentage ± SD of $BrdU^+$ cells (n = 8). (**E**) Expression level of c-Kit on K^+G^- AML cells after 12 hours of cytokine stimulation. Representative histograms are shown in the left panel. Shaded histogram: nonstained AML cells; dotted line: *Raptor*$^{fl/fl}$*CreER*$^{-TAM}$ AML cells; solid line: *Raptor*$^{fl/fl}$*CreER*$^{+TAM}$ AML cells. Data in the right panel are the mean percentage ± SD of MFI of c-Kit (n = 3). For **B**–**E**, **P < 0.01 (Student's t test).

(32, 33), neither *Raptor* deficiency nor rapamycin resulted in hyperphosphorylation of AKT (S473) (Figure 6A and Supplemental Figure 8D). These data suggest that the feedback loop for AKT inhibition through mTORC1 might not occur in these AML cells.

Although mTORC1 reportedly controls cell size (cell growth) (34), we did not observe a decrease in the size of our *Raptor*-deficient AML cells (Figure 6B), and we found that the amount of protein per cell was comparable in control and *Raptor*-deficient AML stem cells (Figure 6, C and D). Inactivation of mTORC1 is also reported to suppress cap-dependent protein translation by enhancing binding between 4E-BP1 and eIF4E (35, 36). Consistent with this, the hypophosphorylation of 4E-BP1 induced by *Raptor* deficiency enhanced binding of 4E-BP1 to eIF4E, which binds the 7-methyl-guanosine cap structure, as determined by a 7-methyl GTP pull-down assay (Figure 6E). We also found an unexpected elevation of eIF4E expression in *Raptor*-deficient AML cells (Figure 6E), and binding of eIF4E to the cap structure appeared to be enhanced. These data suggest that increased production of eIF4E may overcome the inactivation of eIF4E by 4E-BP1.

Raptor-deficient AML stem cells show defective leukemia-initiating capacity. To evaluate the leukemia-initiating capacity of *Raptor*-deficient AML stem cells, we transplanted into recipient mice a limiting dilution series of K^+G^- AML cells isolated from *Raptor*$^{fl/fl}$*CreER* AML mice that had been injected (or not) with TAM. Transplantation of control AML cells promoted efficient development of leukemia with features identical to those of the original AML. Even when only 10 control AML cells were transplanted per mouse, 80% of recipients developed overt AML and died within 60 days (Figure 7A). In contrast, recipients injected with 10 or 100 *Raptor*-deficient AML cells did not die of overt leukemia. Although recipients injected with 1,000 *Raptor*$^{fl/fl}$ *CreER*$^{+TAM}$ AML cells developed leukemia, the emerging AML cells showed incomplete deletion of the *Raptor* gene. Thus, *Raptor* deficiency apparently has a negative impact on leukemia-initiating capacity.

To investigate the effect of *Raptor* deficiency on AML stem cell function, we first evaluated the colony-forming ability of various *Raptor*-deficient AML cell subpopulations in vitro. As expected, the undifferentiated AML cell population (K^+G^- cells) of control AML mice formed colonies at a much higher frequency than did differentiated AML cells (K^-G^+ cells) (Figure 7B). When *Raptor* was deleted by TAM administration, a dramatic reduction was observed in the number of colonies derived from K^+G^- AML cells.

To identify the reason for the failure of colony formation and leukemia propagation by *Raptor*-deficient AML stem cells, we analyzed the behavior of AML cells stimulated with several cytokines, because we assumed that both colony formation and the expansion of leu-

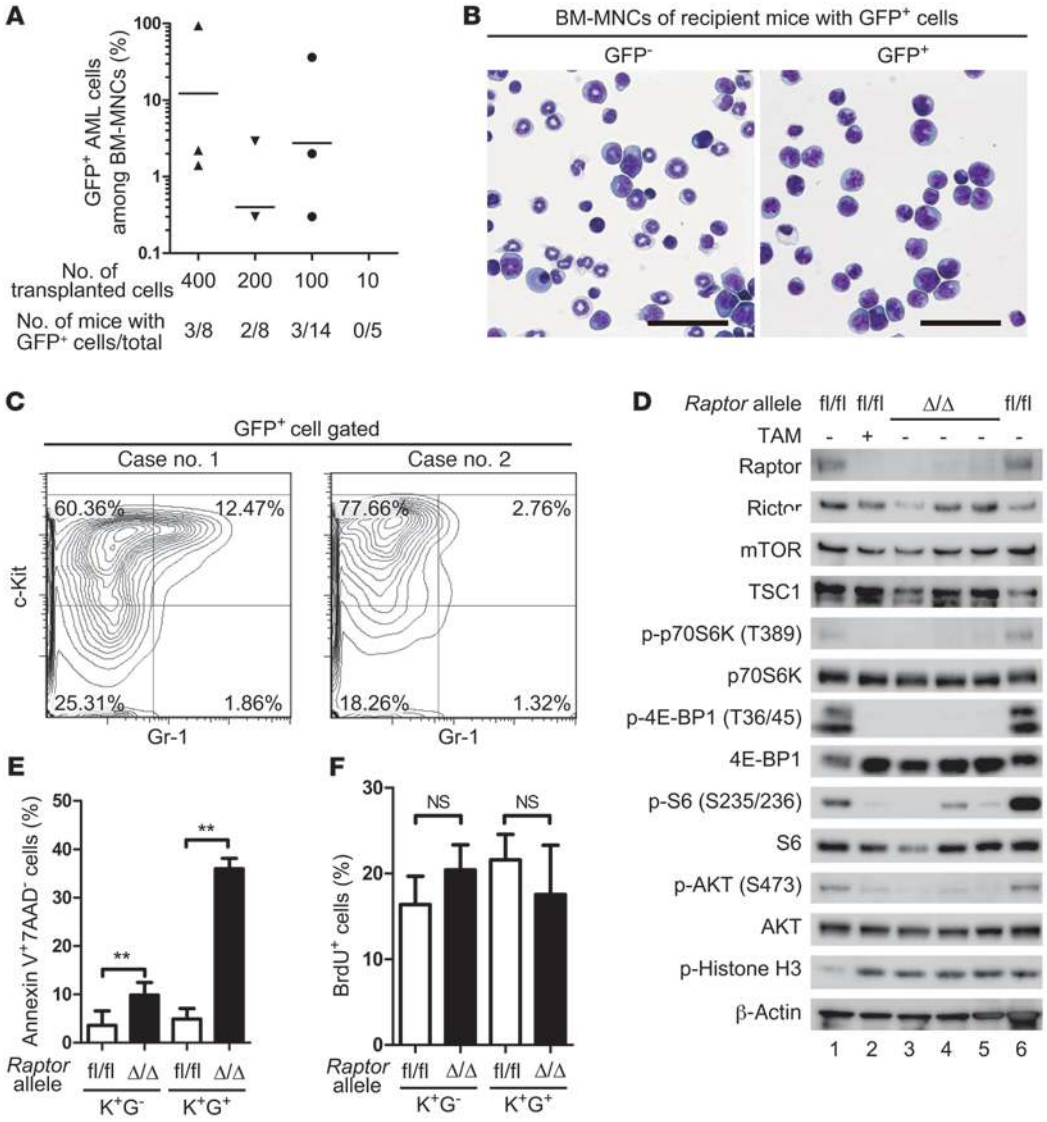

Figure 8

mTORC1-independent long-term survival of AML cells in vivo. (**A**) Presence of AML cells surviving long-term in BM. 10–400 K^+G^- cells from *Raptor*$^{fl/fl}$*CreER*$^{+TAM}$ AML mice were transplanted into recipients, and GFP expression was evaluated in BM-MNCs 100 days after transplantation. Data shown are the percentages of GFP^+ cells among total BM-MNCs. Horizontal lines are the mean percentages of GFP^+ cells in cases where GFP^+ cells were present. Numbers of mice possessing GFP^+ cells/total number of recipients are shown at the bottom of the panel. (**B**) Morphological analysis of *Raptor*$^{\Delta/\Delta}$ AML cells. GFP^- and GFP^+ cells were isolated from BM-MNCs of recipients possessing GFP^+ cells. Cells were stained with May-Grünwald/Giemsa. Scale bars: 50 μm. (**C**) Flow cytometric characterization of the AML cells in **A**. Results of two representative analyses are shown. (**D**) Phosphorylation of mTOR signaling pathway proteins in *Raptor*$^{\Delta/\Delta}$ (long-term *Raptor*-deficient) AML cells. Immunoblotting to detect the indicated proteins was performed on lysates of GFP^+ K^+G^- cells isolated from the following mice: lanes 1 and 6, *Raptor*$^{fl/fl}$*CreER*$^{-TAM}$ AML (fl/fl; TAM–, control); lane 2, *Raptor*$^{fl/fl}$*CreER*$^{+TAM}$ AML at 14 days post-TAM (fl/fl; TAM+); lanes 3–5, *Raptor*$^{\Delta/\Delta}$ AML (Δ/Δ). (**E** and **F**) Analysis of apoptosis and cell cycle in *Raptor*$^{\Delta/\Delta}$ AML cells. The apoptosis rate (**E**) and proportion of cells in the cell cycle (**F**) of the indicated subpopulations from *Raptor*$^{fl/fl}$*CreER*$^{-TAM}$ AML cells (fl/fl; TAM–, control) and *Raptor*$^{\Delta/\Delta}$ AML cells (Δ/Δ) were evaluated by using Annexin V/7AAD staining and BrdU incorporation, respectively. Data shown in **E** and **F** are the mean ± SD of Annexin V^+7AAD^- cells ($n = 4$) and $BrdU^+$ cells ($n = 4$), respectively. $^{**}P < 0.01$ (Student's *t* test).

kemia cells are supported by cytokine signals. We found that *Raptor*-deficient K^+G^- AML cells stimulated with the cytokines SCF, IL-3, and IL-6 showed an increase in apoptosis and a decrease in cell division (Figure 7, C and D). However, *Raptor* deficiency did not downregulate c-Kit (Figure 7E). These data indicate that failure of AML propagation when mTORC1 is inactivated is due to enhanced apoptosis and defective proliferation, but not accelerated differentiation.

Raptor-deficient AML stem cells can survive long-term in BM. To confirm that Raptor deficiency completely depletes AML cells after transplantation, we analyzed BM of the recipient mice injected with fewer than 1,000 *Raptor*$^{fl/fl}$*CreER*$^{+TAM}$ AML cells 100 days after transplantation. Surprisingly, we discovered that some recipient mice retained donor-derived leukemia cells (GFP^+) in their BM. Detailed examination revealed that these surviving GFP^+ cells were present

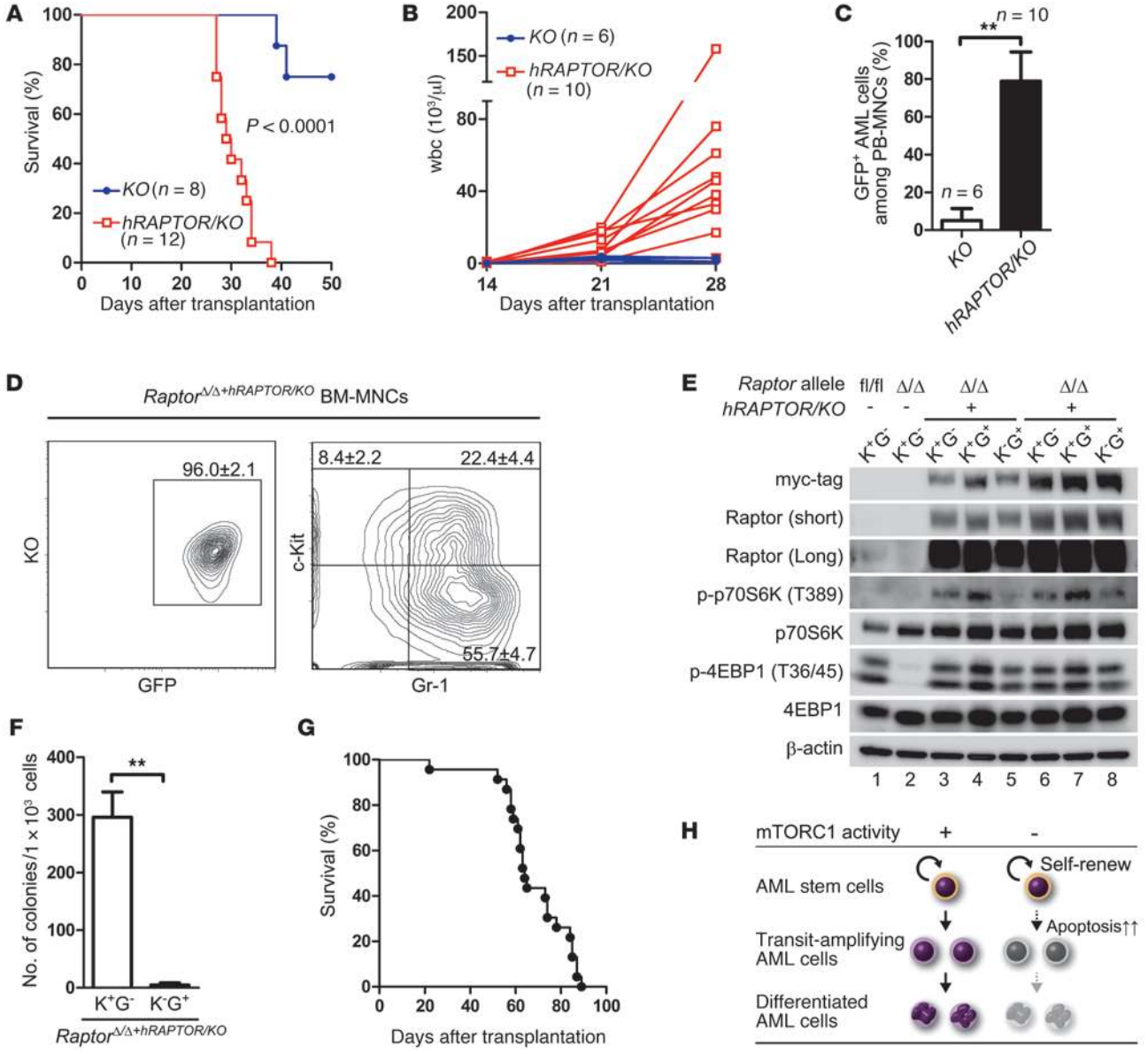

Figure 9

Restoration of leukemia-initiating capacity of long-term *Raptor*-deficient AML stem cells by mTORC1 reactivation. (**A**–**C**) Leukemia development upon restoration of Raptor. Recipient mice were transplanted with BM-MNCs (including $Raptor^{\Delta/\Delta}$ AML cells) infected with either control retrovirus expressing *KO* alone or retrovirus expressing *hRAPTOR* (*hRAPTOR/KO*). Survival (**A**), total number of wbc in PB (**B**), and the mean percentage ± SD of GFP⁺ cells in PB (**C**) of these recipients were analyzed 26–35 days after transplantation. For **A**, the *P* value was determined by the log-rank test. (**D**) Flow cytometric analysis of $Raptor^{\Delta/\Delta+hRAPTOR/KO}$ AML cells. Representative data for GFP/KO fluorescence (left) and c-Kit/Gr-1 expression (right) of BM-MNCs from the recipient mice in **A**–**C** are shown. Values are the mean percentage ± SD of the indicated subpopulations ($n = 7$). (**E**) Phosphorylation of mTOR signaling pathway proteins in $Raptor^{\Delta/\Delta+hRAPTOR/KO}$ AML cells. Immunoblotting to detect the indicated proteins was performed on lysates of the indicated AML cell subpopulations prepared from the following mice: lane 1, $Raptor^{fl/fl}CreER^{-TAM}$ (TAM-, control); lane 2, $Raptor^{\Delta/\Delta}$; lanes 3–5, $Raptor^{\Delta/\Delta+hRAPTOR/KO}$ (case 1); lanes 6–8, $Raptor^{\Delta/\Delta+hRAPTOR/KO}$ (case 2). (**F**) Colony-forming ability of $Raptor^{\Delta/\Delta+hRAPTOR/KO}$ AML cells. K^+G^- or K^-G^+ (GFP^+KO^+) subpopulations isolated from among $Raptor^{\Delta/\Delta+hRAPTOR/KO}$ AML cells were cultured in semisolid medium for 7 days. Data are the mean colony number ± SD ($n = 3$). (**G**) The survival of recipient mice transplanted with 100 K^+G^- $Raptor^{\Delta/\Delta+hRAPTOR/KO}$ AML cells was monitored ($n = 23$). (**H**) Model of the role of mTORC1 in AML stem cell regulation. See text for explanation. $^{**}P < 0.01$ (Student's *t* test).

in 8 of 30 recipients injected with 100–400 $Raptor^{fl/fl}CreER^{+TAM}$ AML cells (Figure 8A) and that the frequency of these leukemia cells in the BM of individuals was highly variable. The GFP⁺ cells were morphologically leukemic (Figure 8B). Interestingly, these animals showed no overt abnormalities of hematopoiesis in PB (Supplemental Figure 9, A and B). Recipient mice injected with only 10 $Raptor^{fl/fl}CreER^{+TAM}$ AML cells did not harbor any leukemia cells at 100 days after transplantation.

The AML cells that survived long-term in recipient BM exhibited AML stem cell phenotypes, as judged by the expression of cell surface markers (i.e., they were K^+G^-; Figure 8C). We confirmed that AML cells surviving long-term showed complete deletion of the *Raptor* gene and loss of the Raptor protein, and we refer to them as $Raptor^{\Delta/\Delta}$ AML cells (Figure 8D). $Raptor^{\Delta/\Delta}$ AML cells showed less phosphorylation of the mTORC1 target molecules p70S6K and 4E-BP1 (Figure 8D). Notably, extended survival of $Raptor^{\Delta/\Delta}$ AML cells was dependent on the in vivo microenvironment, as these cells did not form colonies in vitro (data not shown), just as we observed for the original AML cells prior to transplantation (Figure 7B). $Raptor^{\Delta/\Delta}$ AML cells showed increased apoptosis in vivo compared with control $Raptor^{fl/fl}CreER^{-TAM}$ AML cells, particularly in the K^+G^+ population (Figure 8E). The cell cycle status of $Raptor^{\Delta/\Delta}$ AML cells was comparable to that of controls (Figure 8F). These data suggest that AML stem cells lacking mTORC1 activity can survive long-term in the BM, but that the host animal survives because AML cells that propagate and differentiate are eliminated by apoptosis.

The self-renewal capacity of AML stem cells is sustained in the absence of mTORC1 activity. Finally, we asked whether the AML cells that survive long-term in the BM in the absence of mTORC1 activity are genuine AML stem cells. To this end, we devised a strategy to reintroduce Raptor into those $Raptor^{\Delta/\Delta}$ AML cells that survive long-term in vivo without mTORC1 activity. We prepared a retrovirus carrying the *hRAPTOR* gene labeled with Kusabira-Orange (*hRAPTOR/KO*) (Supplemental Figure 10, A–F) and used this vector, or a control retrovirus expressing *KO* alone, to infect total BM-MNCs from recipient mice harboring $Raptor^{\Delta/\Delta}$ AML cells. To avoid the death of $Raptor^{\Delta/\Delta}$ AML cells ex vivo, retroviral infection was performed with minimum incubation, followed by immediate transplantation into fresh recipients. Mice receiving $Raptor^{\Delta/\Delta}$ AML cells expressing the *hRAPTOR/KO* gene ($Raptor^{\Delta/\Delta+hRAPTOR/KO}$ AML cells) developed overt leukemia (Supplemental Figure 10G) and died rapidly (Figure 9A), whereas mice that received AML cells expressing the control *KO* gene did not. Levels of wbc expressing *hRAPTOR/KO* were greatly elevated in affected recipients by day 28 after transplantation (Figure 9, B and C). All GFP^+ AML cells also showed KO fluorescence (i.e., expressed the *hRAPTOR/KO* gene) (Figure 9D). Moreover, $Raptor^{\Delta/\Delta+hRAPTOR/KO}$ AML cells in BM exhibited a pattern of differentiation markers identical to that of control AML cells (Figure 9D), indicating that introduction of the *hRAPTOR* gene fully restored the original AML phenotype. Immunoblotting confirmed that the introduction of the *hRAPTOR/KO* gene had resulted in RAPTOR protein overexpression (Figure 9E). RAPTOR overexpression promoted increased levels of p-p70S6K and restored p–4E-BP1 levels to those seen in the original AML cells. The colony-forming ability of *Raptor*-deficient K^+G^- AML cells was also rescued by reintroduction of RAPTOR protein (Figure 9F). In addition, a sequential transplantation study showed that only 100 RAPTOR-expressing K^+G^- AML cells were required to efficiently generate overt AML in recipient mice, which resulted in their death within 89 days (Figure 9G). This indicates that the leukemia-initiating capacity was fully restored by reactivation of mTORC1. Together with our finding that $Raptor^{\Delta/\Delta}$ AML cells are cycling (Figure 8F), these data indicate that *Raptor*-deficient AML cells can self-renew and serve as AML stem cells.

Discussion

Distinct mechanisms control the tumor initiation and self-renewal properties of CSCs. It has been assumed that CSCs can survive and self-renew, contributing to cancer recurrence, even when a treatment is effective in reducing tumor mass. This is illustrated by the case of chronic myeloid leukemia patients treated with tyrosine kinase inhibitors (37, 38). These findings indicate that it is necessary to distinguish CSC self-renewal activity from tumor-initiating capacity. Here, we demonstrate that although mTORC1 inactivation eliminates AML cells that exhibit properties of transit-amplifying cells and differentiated cells, it does not affect the self-renewal activity of AML stem cells (Figure 9H). On the basis of these findings, we propose that tumor-initiating and -propagating properties should be considered separately from CSC self-renewal activity. Our observations could have substantial impact on investigations of mechanisms that allow residual CSCs to escape cancer treatment and drive tumor recurrence.

Essential role of mTORC1 in AML propagation. Appropriate regulation of survival and proliferation of transit-amplifying tumor cells is required for robust tumor initiation, which is associated with aggressiveness of tumors. In our study, most *Raptor*-deficient AML cells, particularly differentiated AML cells, showed a remarkable increase in apoptosis in vivo. In addition, *Raptor* deficiency led to a defect in proliferation in differentiated AML cells, but not undifferentiated cells. Thus, mTORC1 activity appears to play a critical role in proliferation and survival in vivo mainly in differentiated cells, rather than AML stem cells. Consistent with these in vivo observations, we found that *Raptor* deficiency enhanced apoptosis and reduced proliferation in AML cells stimulated by cytokine signals in vitro. Because AML cells propagate in vivo as transit-amplifying AML cells supported by cytokine signals, these findings suggest that mTORC1 inactivation results in defective AML propagation, leading to prolonged survival of AML mice.

The molecular mechanism of mTORC1-dependent AML propagation is unclear. Although previous studies reported that inhibition of 4E-BP phosphorylation is associated with the induction of apoptosis in tumors (39, 40), it was assumed that other molecules downstream of mTORC1 cooperatively contribute to AML propagation. To understand how mTORC1 supports AML propagation at the molecular level, we performed a quantitative phosphoproteomics study using the SILAC (stable isotope labeling with amino acids in cell culture) method and found numerous peptides that were dramatically de-phosphorylated by *Raptor* deficiency (T. Hoshii and N. Sugiyama, unpublished observations). Among these molecules, there were several known downstream targets of mTORC1, including Raptor, 4E-BP1/2, AKTS1 (also known as PRAS40), and LARP1 (26, 27). Decreased phosphorylation of AKTS1, as well as of 4E-BPs, is reportedly associated with apoptosis in tumor cells (41). Therefore, we assumed that mTORC1 inactivation affects the activities of these target molecules, which are regulated by their phosphorylation status, resulting in defective AML propagation.

Although rapamycin derivatives have been tested in AML patients in clinical trials, it has remained controversial whether such medications are effective (42–44). In our study, rapamycin treatment slightly prolonged the survival of AML mice, but it had a milder effect than *Raptor* deficiency. The difference is likely due to the limited effects of rapamycin on mTORC1 inhibition. We found that the inhibitory effects of rapamycin differed among mTORC1 targets. For example, rapamycin treatment effectively suppressed the phosphorylation of p70S6K but did not affect the phosphorylation of 4E-BP1, which is consistent with previous reports (24, 25). These data strongly suggest that a genetic approach is required to understand the bona fide effects of

mTORC1 inhibition in vivo. Thus, dissection of mTORC1 signaling pathways using the *Raptor*-deficient AML cells should provide critical evidence for identifying indicators or therapeutic targets to control the aggressiveness of leukemic diseases.

Self-renewal of AML stem cells lacking mTORC1. A particularly interesting and unexpected finding emerging from our work is that AML stem cells lacking mTORC1 activity can proliferate and survive long-term in vivo. Previous studies demonstrated that mTORC1 activity plays critical roles in cell proliferation in embryonic fibroblasts and cell lines (45, 46). The knockdown of *Raptor* or a decrease in serum concentration in culture inhibits cell proliferation. Because the proliferation is restored by 4E-BP1/2 deficiency, 4E-BPs are thought to be key regulators of cell proliferation when mTORC1 activity is downregulated (45). As expected, we found that embryonic fibroblasts lacking *Raptor* showed remarkable defects in cell proliferation (Supplemental Figure 1C). However, we unexpectedly observed that the cell cycle and self-renewing proliferation of AML stem cells in vivo were not altered by mTORC1 inactivation in our experiments. Because the phosphorylation of 4E-BP1 was dramatically suppressed in these cells, 4E-BP1–independent mechanisms of cell proliferation must support self-renewal of AML stem cells. Although 4E-BP1 phosphorylation reportedly induces cap-dependent protein translation, which controls the growth of individual cells, we found no evidence of an inhibitory effect of *Raptor* deficiency on the size or protein amount of AML stem cells. We confirmed that *Raptor* deficiency enhanced binding of 4E-BP1 to eIF4E due to 4E-BP1 hypophosphorylation. However, we unexpectedly found elevated eIF4E protein levels and enhanced eIF4E binding to cap structures in *Raptor*-deficient AML cells. Because eIF4E overexpression reportedly increases cell size and resistance to rapamycin treatment (41, 42), the increased presence of eIF4E protein on cap structures may compensate for the inhibition of eIF4E activity by 4E-BP1, leading to the retained cell growth and self-renewal in the absence of mTORC1.

Similar to what we observed in AML stem cells, we also found that *Raptor* deficiency did not cause defective phenotypes in GMP myeloid progenitor cells. Because AML stem cells likely originate from myeloid progenitors, the two types of cells may share the property of mTORC1 dependency (22). A possible compensatory mechanism for cell proliferation observed in *Raptor*-deficient GMP is mTORC1-independent regulation of the ribosomal protein S6 and eEF2K. Although S6 and eEF2K are substrates of p70S6K, it was also reported that p90 RSK can phosphorylate these proteins (28, 30). Activation of p90 RSK is dependent on Ras/ERK signaling. Study of hematopoietic progenitor cells with the K-ras^{G12D} mutation revealed that phosphorylation of S6 after GM-CSF stimulation is highly dependent on MEK/ERK signaling, but not on PI3K/AKT signaling (29). Therefore, such mTORC1-independent S6 and eEF2K phosphorylation may compensate for the lack of mTORC1 in supporting cell proliferation of GMPs. Unlike in GMPs, the phosphorylation of S6 was strongly inhibited in *Raptor*-deficient AML stem cells. However, the residual level of S6 activity supported by mTORC1-independent signaling may be enough to promote the self-renewal of AML stem cells.

It has been reported that mTORC1 inhibition activates autophagy, a protein degradation system, to generate energy for survival under conditions of stress or starvation (4). An interaction of Raptor and ULK1 mediates the incorporation of mTORC1 into the ULK1-Atg13-FIP200 complex, which is required for autophagy, and mTOR phosphorylates ULK1 and Atg13, indicating that autophagy is directly regulated by mTORC1 (47). Therefore, autophagy induced by *Raptor* deficiency may support the survival of AML stem cells in vivo. In our preliminary experiments, we did not observe an increase in LC3-II in *Raptor*-deficient AML stem cells (our unpublished observations). Thus, the roles of autophagy in AML stem cell survival are unclear in our experiments. We believe that it is necessary to investigate how autophagy is involved in the survival of AML stem cells, because such information may be important for developing a strategy to use a combination of mTORC1 and autophagy inhibitors to eradicate AML stem cells.

A recent study revealed that AKT is a key regulator for the maintenance of AML stem cells (48). Suppression of AKT activity is reported to be essential for inhibiting the differentiation of leukemia stem cells and supporting their self-renewal ability in MLL-AF9–driven AML. Feedback activation of the PI3K/AKT pathway is triggered by inhibition of Grb10 and/or activation of IRS after acute mTORC1 inactivation (26, 27). On the other hand, prolonged rapamycin treatment is reported to suppress AKT via the disassembly of the mTORC2 complex in certain cell types (49). In our study, we observed that AKT phosphorylation was attenuated in *Raptor*$^{\Delta/\Delta}$ AML cells. We found that *Raptor* deficiency did not affect the expression level of Rictor, an essential component of mTORC2, but it is possible that long-term inactivation of mTORC1 in *Raptor*-deficient AML cells affects the assembly and activity of mTORC2, leading to inhibition of AKT, in the same manner as prolonged rapamycin treatment (49). To investigate whether mTORC2 is involved in regulating AKT for the survival of AML stem cells, a genetic study using *mTOR* or *Rictor* mutant mice would be necessary. Thus, although the mechanism is unclear, the suppression of AKT in *Raptor*$^{\Delta/\Delta}$ AML stem cells may suppress the differentiation of AML stem cells and support their self-renewal activity.

Our results also suggest that mTORC1 inactivation might prevent the differentiation of AML stem cells in a cell-intrinsic manner, because we found that *Raptor*-deficient AML cells had higher c-Kit expression than controls in culture (Figure 7E). Unknown microenvironmental factors may enhance this effect of mTORC1, because we observed a remarkable increase in the absolute number of AML stem cells in vivo (Figure 5E). These findings lead to the intriguing idea that mTORC1 inhibition enhances self-renewal activity in combination with microenvironmental factors. Further dissection of the regulation of *Raptor*-deficient AML stem cells is required to identify the critical factors or functions of AML stem cells. Increased understanding of the mechanisms by which AML stem cells self-renew should suggest novel therapeutic approaches that will successfully eradicate CSCs.

Methods

Mice. To generate mice bearing an inducible conditional deletion of *Raptor*, we obtained BAC clones (BACPAC Resources Center) that encode the mouse genomic DNA sequences encompassing the region containing exon 2 of the *Raptor* gene. Genomic DNA fragments were inserted into a plasmid containing paired loxP sites and FRT recombination sites flanking a neomycin selection cassette. A diphtheria toxin cassette was added downstream of the 3′ arm to reduce the frequency of random insertion. This vector was transfected into feeder-free TT2 ES cells (derived from the TT2 ES cell line; ref. 50) by electroporation, and the cells were subjected to G418 selection as previously described (51). ES clones possessing the recombined allele were identified by PCR and Southern blot analyses. ES cells were aggregated with ICR morulae, and chimeras were obtained. The chimeric mice were crossed with *CAG-Flp* mice (51) to remove the neo cassette and generate mice with

the *Raptor*^{fl} allele. Mice with the *Raptor*^{fl} allele were crossed with *Rosa26-CreER*^{T2} mice (52) obtained from Tyler Jacks (Massachusetts Institute of Technology, Cambridge, Massachusetts, USA), and the resulting progeny were backcrossed for at least 6 generations onto the C57BL/6-CD45.2 genetic background. All mice used as transplantation recipients in this study were 8- to 12-week-old C57BL/6-CD45.1 mice (Sankyo Lab).

PCR primers. The primers used to identify the *Raptor* WT, floxed, and deleted alleles in PCR analyses were raptor-a (AAAGACAAACCAGTGAGCAAGGGG), raptor-b (GGAGCTTCCTTATCGTGAATCTCC), and raptor-c (CTGGGAACTGCGATAAGCCG).

Blood collection and analysis. Total BM cells were obtained from femoral and tibial bones by aspiration. MNCs were isolated from total BM cells by density gradient centrifugation using Lymphoprep (Axis-Shield). PB cells were collected from the postorbital vein and suspended in diluted heparin solution. Blood counts were performed using Celltac (NIHON KOHDEN). MNCs in PB were isolated by dextran sedimentation and ammonium chloride lysis of erythrocytes using standard procedures.

Tamoxifen and rapamycin treatments. To analyze the effect of *Raptor* deficiency in mice without transplantation, we treated 8-week-old mice with TAM (Sigma-Aldrich). TAM was dissolved in corn oil (Sigma-Aldrich) to 20 mg/ml and injected i.p. at 150 mg/kg/d for 5 consecutive days. The corn oil diluent was injected as the control. For TAM treatment of cells in vitro, 1 μM 4-hydroxytamoxifen (4-OHT; Sigma-Aldrich) was added to the culture medium. Rapamycin (Sirolimus, LC Laboratories) was dissolved in ethanol to 10 mg/ml stock solution. For in vivo experiments, the rapamycin stock solution was diluted to make a final concentration of 0.4 mg/ml rapamycin in 5% PEG-400, 5% Tween 80, and 4% ethanol. Rapamycin (4 mg/kg) or vehicle (5% PEG-400, 5% Tween 80, and 4% ethanol) was injected i.p. every other day. For rapamycin treatment of cells in vitro, 100 nM rapamycin (Cell Signaling Technology) dissolved in methanol was added to the culture medium.

Flow cytometry. mAbs recognizing the following markers were used for flow cytometry: Sca-1 (E13-161.7), CD4 (L3T3), CD8 (clone 53-6.7), B220 (RA3-6B2), TER119 (Ly-76), Gr-1 (RB6-8C5), Mac-1 (M1/70), IL-7Rα chain (B12-1), FcγIII/II receptor (2.4G2), CD34 (RAM34), IgM (II/41), CD45.1 (A20), CD45.2 (clone 104), and c-Kit (2B8) (all from BD Biosciences or eBiosciences). Marker analyses were performed using a FACSCanto II (BD Biosciences), and cell sorting was performed using a FACSAria (BD Biosciences).

For analysis of intracellular phosphorylated proteins, 5×10^4 cells were fixed in 4% paraformaldehyde at 37°C for 10 minutes and permeabilized in 90% cold methanol for at least 30 minutes. Cells were then washed with staining buffer (5% FBS in PBS) and incubated at room temperature for 1 hour with Alexa Fluor 647–conjugated anti–p-S6 (S235/236) plus Alexa Fluor 488–conjugated anti–p-4E-BP1 (T37/46; T36/T45 for *Mus musculus*) Abs, or Alexa Fluor 647–conjugated rabbit mAb IgG isotype control and Alexa Fluor 488–conjugated rabbit mAb IgG isotype control. Immunostained cells were washed with staining buffer and analyzed by flow cytometry.

Colony-forming assay. $K^+S^+L^-$ cells and GMPs isolated from BM of non-AML mice, or $GFP^+K^+G^-$ or K^-G^+ cells isolated from BM of AML mice, were cultured for 10 or 7 days, respectively, in semisolid medium containing 50 ng/ml recombinant murine stem cell factor (rmSCF), 10 ng/ml rmIL-3, 10 ng/ml rmIL-6, and 3 U/ml recombinant human erythropoietin (rhEPO) (Methocult GF M3434, Stem Cell Technologies) at 37°C in humidified air containing 5% CO_2. Colonies containing more than 40 cells were counted under a microscope.

Cell cycle. To analyze the cell cycle of hematopoietic cells in vivo, BrdU (100 mg/kg; Sigma-Aldrich) was injected i.p. into mice. After 2 hours, cells were collected, immunostained to detect surface markers, and purified using a cell sorter. For analysis of the cell cycle of AML cells in vitro, cells were cultured with medium supplemented with 10 μM BrdU for 30 minutes. Cells were fixed in 70% ethanol at –30°C for 16 hours. The DNA in fixed cells was denatured by treatment with 2 N HCl at room temperature for 30 minutes, followed by neutralization using 0.05 M borax buffer. Incorporated BrdU was labeled by incubation with FITC-conjugated anti-BrdU Ab (BD Biosciences) at room temperature for 1 hour. Labeled cells were resuspended in PBS containing 1% bovine serum albumin and 7-aminoactinomycin D (7AAD; BD Biosciences) plus RNase A (Sigma-Aldrich), and BrdU-positive cells were quantified by flow cytometry.

Apoptosis. For TUNEL assays of floating cells, cells were fixed in 4% paraformaldehyde and permeabilized in 70% ethanol at –30°C for 16 hours. For TUNEL assays of small intestine, small intestines were fixed with 4% paraformaldehyde, and paraffin-embedded tissues were sectioned, dewaxed, and rehydrated. Fragmented DNA was labeled with fluorescein-12-dUTP using the DeadEnd Fluorometric TUNEL System (Promega) and analyzed by flow cytometry or FV1000 confocal microscopy (Olympus). For Annexin V staining, cells were incubated with PE-conjugated Annexin-V and 7AAD in Annexin V binding buffer (BD Biosciences) in accordance with the manufacturer's protocol.

Competitive repopulation assay in vivo. Tester BM-MNCs (1×10^6) from *Raptor*$^{fl/fl}$ or *Raptor*$^{fl/fl}$*CreER* mice (CD45.2) and competitor WT BM-MNCs (1×10^6, CD45.1/2) were transplanted into lethally irradiated (9.5 Gy) recipient mice ($CD45.1^+$). At 8 weeks after transplantation, TAM was administered to the recipients as described above. Hematopoietic cells regenerated from tester cells or competitor cells were examined by flow cytometry.

Gene transduction by retroviral infection. The pMSCV-*MLL-AF9*-ires-*eGFP* vector was a gift from Akihiko Yokoyama, Kyoto University, Kyoto, Japan. The Myc-tagged human *RAPTOR* gene was a gift from David M. Sabatini, Whitehead Institute, Cambridge, Massachusetts, USA (Addgene plasmid 1859) and was cloned into the pGCDNsam-ires-*eGFP* or pGCDNsam-ires-*hKO* vector (both gifts from Masafumi Onodera, National Center for Child Health and Development, Tokyo, Japan). Retroviral packaging cells (Plat-E, ref. 53; gift from Toshio Kitamura, University of Tokyo, Tokyo, Japan) were transiently transfected with the above plasmids using calcium phosphate, and culture supernatants containing retroviruses were collected 48 hours after transfection.

For retroviral gene transduction, three cell type–specific protocols were used: (a) $K^+S^+L^-$ cells isolated from *Raptor*$^{fl/fl}$ or *Raptor*$^{fl/fl}$*CreER* mice were cultured overnight in serum-free S-Clone SF-03 medium (Sanko Junyaku) supplemented with 100 ng/ml recombinant human thrombopoietin (PeproTech) plus 100 ng/ml rmSCF (Wako Pure Chemical). Cells were then infected with retroviruses carrying *MLL-AF9*-ires-*eGFP* or *hRAPTOR*-ires-*eGFP* using CombiMag (OZ Biosciences) in accordance with the manufacturer's instructions. (b) AML cells were cultured for several days in RPMI 1640 medium supplemented with 10% FBS and 10 ng/ml rmIL-3 (Wako Pure Chemical). Cells were infected with a retroviral vector carrying *hRAPTOR*-ires-*hKO* using 8 μg/ml Polybrene. Two days after infection, KO^+ cells were collected using a cell sorter and subjected to colony-forming assays as described above. (c) For *Raptor*$^{\Delta/\Delta}$ AML cells, freshly isolated BM cells from recipient mice possessing *Raptor*$^{\Delta/\Delta}$ AML cells were suspended in RPMI 1640 medium supplemented with 20 ng/ml rmSCF, 10 ng/ml rmIL-3, 10 ng/ml rmIL-6, and 10 ng/ml rmIL-7 and containing 8 μg/ml Polybrene. Spin infection was performed by adding retrovirus carrying *hRAPTOR*-ires-*KO* or *KO* to the suspended cells and centrifuging at 1,500 *g* for 1 hour. After a first round of spin infection, cells underwent a second round of spin infection using fresh retrovirus. Then, 2×10^6 infected cells were cultured for an additional 2 hours before transplantation into lethally irradiated (9.5 Gy) syngeneic recipient mice.

Murine AML model. $K^+S^+L^-$ cells isolated from *Raptor*$^{fl/fl}$, *Raptor*$^{+/+}$*CreER*, or *Raptor*$^{fl/fl}$*CreER* mice were infected with retrovirus carrying *MLL-AF9*-ires-*eGFP* as described above and transplanted into lethally irradiated syngeneic mice along with 2×10^5 normal BM-MNCs (rescue cells). AML-

like disease developed in these AML mice between 34 and 124 days after transplantation (mean, 76.7 days; SD, 27.8). After the appearance of AML symptoms, 5×10^5 BM-MNCs from the AML mice were transplanted intravenously into lethally irradiated syngeneic recipients along with 5×10^5 normal BM-MNCs. Administration of TAM (150 mg/kg/d for 5 days, i.p.) was begun 3 days after transplantation. Corn oil was injected as the diluent control in the same manner. For the limiting dilution transplantation assay to evaluate leukemia-initiating capacity, $GFP^+c\text{-}Kit^+Gr\text{-}1^-$ AML cells were collected from recipient mice 14 days after the last TAM injection and transplanted into lethally irradiated syngeneic recipients along with 2×10^5 normal BM-MNCs.

Immunoblotting. Cells (5×10^4) of various subpopulations were purified by cell sorting and lysed in SDS sample buffer containing proteinase inhibitor (P8340, Sigma-Aldrich), phosphatase inhibitor cocktail 2 (P5726, Sigma-Aldrich), and phosphatase inhibitor cocktail 3 (P0044, Sigma-Aldrich). Lysis was completed via ultrasonication, and proteins were denatured by boiling. Denatured proteins were separated on a 5%–20% acrylamide gradient gel and transferred to a PVDF membrane (GE Healthcare). Blots were incubated with Abs against Raptor, mTOR, Rictor, TSC1, p–4E-BP1 (T37/46; T36/T45 for *M. musculus*), p–4E-BP1 (S65; S64 for *M. musculus*), p–4E-BP1 (T70; T69 for *M. musculus*), 4E-BP1, p-S6 (S235/236), p-S6 (S240/244), S6, p-p70S6K (T389), p70S6K, p-AKT (T308), p-AKT (S473), and eIF4E (all from Cell Signaling Technologies), p–histone H3 (Upstate), β-actin (Sigma-Aldrich), and Myc tag (MBL). Immunocomplexes were labeled using an HRP-conjugated anti-mouse Ab (GE Healthcare) or anti-rabbit Ab (Cell Signaling Technology) and visualized using Immunostar LD (Wako) with ImageQuant LAS 4000 (GE Healthcare).

Histochemical staining. For May-Grünwald/Giemsa staining, cells purified by cell sorting were centrifuged onto glass slides and stained with May-Grünwald solution (MUTO Pure Chemicals) for 3 minutes. Subsequently, the slides were washed with distilled water for 3 minutes and stained with Giemsa solution (MUTO Pure Chemicals) for 10 minutes. For hematoxylin & eosin staining, rehydrated paraffin-embedded tissue sections were stained with Mayer's hematoxylin solution (Wako) for 5 minutes and washed with water for 5 minutes. The slides were then stained with eosin solution (Wako) for 10 seconds. Cells and tissues were visualized with Axio Imager A1 microscopes (Zeiss).

Protein quantification. For the colorimetric detection and quantification of total protein, cells (5×10^5) were purified by cell sorting and lysed in Cell Lysis Buffer (Cell Signaling Technology) containing proteinase inhibitor (P8340, Sigma-Aldrich). Lysis was completed via ultrasonication and quantified with bicinchoninic acid (BCA) protein assay reagent (Pierce). For silver staining of protein, cells (5×10^4) were lysed in SDS sample buffer containing proteinase inhibitor and phosphatase inhibitor cocktail. Denatured proteins were separated in a 5%–20% acrylamide gradient gel and then stained with a Silver Stain II Kit *Wako* (Wako).

7-methyl GTP pull-down assay. Cells (1×10^6) from each population were collected by cell sorter and lysed with lysis buffer (50 mM Tris pH 7.5, 150 mM KCl, 5 mM 2-ME, 1 mM EDTA, proteinase inhibitor, phosphatase inhibitor). The samples were completely lysed via ultrasonication and incubated with 7-methyl GTP-Sepharose 4B beads (GE Healthcare) at 4°C. After 16 hours of incubation, the beads were washed twice with lysis buffer. The beads were suspended in SDS sample buffer and denatured by boiling. Precipitated proteins were detected by Western blot analysis, and the 4E-BP1/eIF4E ratio was measured using ImageJ software (http://rsbweb.nih.gov/ij/).

Statistics. Statistical differences were determined using the unpaired Student's *t*-test (2-tailed) for *P*-values, and the log-rank (Mantel-Cox) test for survival curves.

Study approval. Animal care was in accordance with the guidelines for animal and recombinant DNA experiments of Kanazawa University or Kumamoto University. Animal studies were approved by the Committee on Animal Experimentation of Kanazawa University and the Ethics Committee of the Center for Animal Resources and Development, Kumamoto University.

Acknowledgments

We thank Tyler Jacks for providing *Rosa26-CreER^{T2}* mice; Akihiko Yokoyama for the pMSCV-*MLL-AF9*-ires-*eGFP* vector; Masafumi Onodera for the pGCDNsam-ires-*eGFP* and pGCDNsam-ires-*hKO* vectors; Toshio Kitamura for Plat-E retroviral packaging cells; Minoru Terashima for technical advice; and Miyako Takegami, Kazue Sawa, and Yumi Sakumura for expert technical support. We also thank members of the Hirao laboratory for helpful discussions. T. Hoshii was supported by a Grant-in-Aid for Young Scientists (B) and a Grant-in-Aid for Scientific Research on Innovative Areas "Cell Fate" from the Ministry of Education, Culture, Sports, Science and Technology, Japan. A. Hirao was supported by a Grant-in-Aid for Scientific Research on Innovative Areas and the Project for Development of Innovative Research on Cancer Therapeutics (P-DIRECT) from the Ministry of Education, Culture, Sports, Science and Technology, Japan, and by a grant from the Japan Science and Technology Agency (JST), Core Research for Evolution Science and Technology (CREST).

Received for publication December 5, 2011, and accepted in revised form April 4, 2012.

Address correspondence to: Atsushi Hirao, Division of Molecular Genetics, Cancer and Stem Cell Research Program, Cancer Research Institute, Kanazawa University, Kakuma-machi, Kanazawa, Ishikawa 920-1192, Japan. Phone: 81762646755; Fax: 81762344508; E-mail: ahirao@staff.kanazawa-u.ac.jp.

1. Ma XM, Blenis J. Molecular mechanisms of mTOR-mediated translational control. *Nat Rev Mol Cell Biol*. 2009;10(5):307–318.
2. Ramanathan A, Schreiber SL. Direct control of mitochondrial function by mTOR. *Proc Natl Acad Sci U S A*. 2009;106(52):22229–22232.
3. Cunningham JT, Rodgers JT, Arlow DH, Vazquez F, Mootha VK, Puigserver P. mTOR controls mitochondrial oxidative function through a YY1-PGC-1alpha transcriptional complex. *Nature*. 2007;450(7170):736–740.
4. Rabinowitz JD, White E. Autophagy and metabolism. *Science*. 2010;330(6009):1344–1348.
5. Alessi DR, Pearce LR, Garcia-Martinez JM. New insights into mTOR signaling: mTORC2 and beyond. *Sci Signal*. 2009;2(67):pe27.
6. Guertin DA, et al. Ablation in mice of the mTORC components raptor, rictor, or mLST8 reveals that mTORC2 is required for signaling to Akt-FOXO and PKCalpha, but not S6K1. *Dev Cell*. 2006;11(6):859–871.
7. Jacinto E, et al. SIN1/MIP1 maintains rictor-mTOR complex integrity and regulates Akt phosphorylation and substrate specificity. *Cell*. 2006;127(1):125–137.
8. Polak P, Cybulski N, Feige JN, Auwerx J, Ruegg MA, Hall MN. Adipose-specific knockout of raptor results in lean mice with enhanced mitochondrial respiration. *Cell Metab*. 2008;8(5):399–410.
9. Bentzinger CF, et al. Skeletal muscle-specific ablation of raptor, but not of rictor, causes metabolic changes and results in muscle dystrophy. *Cell Metab*. 2008;8(5):411–424.
10. Chen C, Liu Y, Liu R, Ikenoue T, Guan KL, Zheng P. TSC-mTOR maintains quiescence and function of hematopoietic stem cells by repressing mitochondrial biogenesis and reactive oxygen species. *J Exp Med*. 2008;205(10):2397–2408.
11. Gan B, et al. mTORC1-dependent and -independent regulation of stem cell renewal, differentiation, and mobilization. *Proc Natl Acad Sci U S A*. 2008;105(49):19384–19389.
12. Lee JY, et al. mTOR activation induces tumor suppressors that inhibit leukemogenesis and deplete hematopoietic stem cells after Pten deletion. *Cell Stem Cell*. 2010;7(5):593–605.
13. Nardella C, et al. Aberrant Rheb-mediated mTORC1 activation and Pten haploinsufficiency are cooperative oncogenic events. *Genes Dev*. 2008;22(16):2172–2177.
14. Yilmaz OH, et al. Pten dependence distinguishes

haematopoietic stem cells from leukaemia-initiating cells. *Nature*. 2006;441(7092):475–482.
15. Zhang J, et al. PTEN maintains haematopoietic stem cells and acts in lineage choice and leukaemia prevention. *Nature*. 2006;441(7092):518–522.
16. Reya T, Morrison SJ, Clarke MF, Weissman IL. Stem cells, cancer, and cancer stem cells. *Nature*. 2001;414(6859):105–111.
17. Somervaille TC, Cleary ML. Identification and characterization of leukemia stem cells in murine MLL-AF9 acute myeloid leukemia. *Cancer Cell*. 2006;10(4):257–268.
18. Krivtsov AV, et al. Transformation from committed progenitor to leukaemia stem cell initiated by MLL-AF9. *Nature*. 2006;442(7104):818–822.
19. Huntly BJ, et al. MOZ-TIF2, but not BCR-ABL, confers properties of leukemic stem cells to committed murine hematopoietic progenitors. *Cancer Cell*. 2004;6(6):587–596.
20. Cozzio A, Passegue E, Ayton PM, Karsunky H, Cleary ML, Weissman IL. Similar MLL-associated leukemias arising from self-renewing stem cells and short-lived myeloid progenitors. *Genes Dev*. 2003;17(24):3029–3035.
21. Lavau C, Luo RT, Du C, Thirman MJ. Retrovirus-mediated gene transfer of MLL-ELL transforms primary myeloid progenitors and causes acute myeloid leukemias in mice. *Proc Natl Acad Sci U S A*. 2000;97(20):10984–10989.
22. Goardon N, et al. Coexistence of LMPP-like and GMP-like leukemia stem cells in acute myeloid leukemia. *Cancer Cell*. 2011;19(1):138–152.
23. Somervaille TC, et al. Hierarchical maintenance of MLL myeloid leukemia stem cells employs a transcriptional program shared with embryonic rather than adult stem cells. *Cell Stem Cell*. 2009; 4(2):129–140.
24. Wang X, Beugnet A, Murakami M, Yamanaka S, Proud CG. Distinct signaling events downstream of mTOR cooperate to mediate the effects of amino acids and insulin on initiation factor 4E-binding proteins. *Mol Cell Biol*. 2005;25(7):2558–2572.
25. Choo AY, Yoon SO, Kim SG, Roux PP, Blenis J. Rapamycin differentially inhibits S6Ks and 4E-BP1 to mediate cell-type-specific repression of mRNA translation. *Proc Natl Acad Sci U S A*. 2008;105(45):17414–17419.
26. Hsu PP, et al. The mTOR-regulated phosphoproteome reveals a mechanism of mTORC1-mediated inhibition of growth factor signaling. *Science*. 2011;332(6035):1317–1322.
27. Yu Y, et al. Phosphoproteomic analysis identifies Grb10 as an mTORC1 substrate that negatively regulates insulin signaling. *Science*. 2011; 332(6035):1322–1326.
28. Roux PP, et al. RAS/ERK signaling promotes site-specific ribosomal protein S6 phosphorylation via RSK and stimulates cap-dependent translation. *J Biol Chem*. 2007;282(19):14056–14064.
29. Van Meter ME, et al. K-RasG12D expression induces hyperproliferation and aberrant signaling in primary hematopoietic stem/progenitor cells. *Blood*. 2007;109(9):3945–3952.
30. Wang X, Li W, Williams M, Terada N, Alessi DR, Proud CG. Regulation of elongation factor 2 kinase by p90(RSK1) and p70 S6 kinase. *EMBO J*. 2001;20(16):4370–4379.
31. Wang Y, et al. The Wnt/beta-catenin pathway is required for the development of leukemia stem cells in AML. *Science*. 2010;327(5973):1650–1653.
32. O'Reilly KE, et al. mTOR inhibition induces upstream receptor tyrosine kinase signaling and activates Akt. *Cancer Res*. 2006;66(3):1500–1508.
33. Sun SY, et al. Activation of Akt and eIF4E survival pathways by rapamycin-mediated mammalian target of rapamycin inhibition. *Cancer Res*. 2005;65(16):7052–7058.
34. Kim DH, et al. mTOR interacts with raptor to form a nutrient-sensitive complex that signals to the cell growth machinery. *Cell*. 2002;110(2):163–175.
35. Brunn GJ, et al. Phosphorylation of the translational repressor PHAS-I by the mammalian target of rapamycin. *Science*. 1997;277(5322):99–101.
36. Beretta L, Gingras AC, Svitkin YV, Hall MN, Sonenberg N. Rapamycin blocks the phosphorylation of 4E-BP1 and inhibits cap-dependent initiation of translation. *EMBO J*. 1996;15(3):658–664.
37. Michor F, et al. Dynamics of chronic myeloid leukaemia. *Nature*. 2005;435(7046):1267–1270.
38. Roeder I, Horn M, Glauche I, Hochhaus A, Mueller MC, Loeffler M. Dynamic modeling of imatinib-treated chronic myeloid leukemia: functional insights and clinical implications. *Nat Med*. 2006;12(10):1181–1184.
39. Nishioka C, Ikezoe T, Yang J, Yokoyama A. Inhibition of MEK/ERK signaling induces apoptosis of acute myelogenous leukemia cells via inhibition of eukaryotic initiation factor 4E-binding protein 1 and down-regulation of Mcl-1. *Apoptosis*. 2010;15(7):795–804.
40. She QB, et al. 4E-BP1 is a key effector of the oncogenic activation of the AKT and ERK signaling pathways that integrates their function in tumors. *Cancer Cell*. 2010;18(1):39–51.
41. Madhunapantula SV, Sharma A, Robertson GP. PRAS40 deregulates apoptosis in malignant melanoma. *Cancer Res*. 2007;67(8):3626–3636.
42. Recher C, et al. Antileukemic activity of rapamycin in acute myeloid leukemia. *Blood*. 2005; 105(6):2527–2534.
43. Rizzieri DA, et al. A phase 2 clinical trial of deforolimus (AP23573, MK-8669), a novel mammalian target of rapamycin inhibitor, in patients with relapsed or refractory hematologic malignancies. *Clin Cancer Res*. 2008;14(9):2756–2762.
44. Yee KW, et al. Phase I/II study of the mammalian target of rapamycin inhibitor everolimus (RAD001) in patients with relapsed or refractory hematologic malignancies. *Clin Cancer Res*. 2006;12(17):5165–5173.
45. Dowling RJ, et al. mTORC1-mediated cell proliferation, but not cell growth, controlled by the 4E-BPs. *Science*. 2010;328(5982):1172–1176.
46. Fingar DC, Richardson CJ, Tee AR, Cheatham L, Tsou C, Blenis J. mTOR controls cell cycle progression through its cell growth effectors S6K1 and 4E-BP1/eukaryotic translation initiation factor 4E. *Mol Cell Biol*. 2004;24(1):200–216.
47. Hosokawa N, et al. Nutrient-dependent mTORC1 association with the ULK1-Atg13-FIP200 complex required for autophagy. *Mol Biol Cell*. 2009;20(7):1981–1991.
48. Sykes SM, et al. AKT/FOXO signaling enforces reversible differentiation blockade in myeloid leukemias. *Cell*. 2011;146(5):697–708.
49. Sarbassov DD, et al. Prolonged rapamycin treatment inhibits mTORC2 assembly and Akt/PKB. *Mol Cell*. 2006;22(2):159–168.
50. Yagi T, et al. A novel ES cell line, TT2, with high germline-differentiating potency. *Anal Biochem*. 1993;214(1):70–76.
51. Taniwaki T, et al. Characterization of an exchangeable gene trap using pU-17 carrying a stop codon-beta geo cassette. *Dev Growth Differ*. 2005;47(3):163–172.
52. Ventura A, et al. Restoration of p53 function leads to tumour regression in vivo. *Nature*. 2007; 445(7128):661–665.
53. Morita S, Kojima T, Kitamura T. Plat-E: an efficient and stable system for transient packaging of retroviruses. *Gene Ther*. 2000;7(12):1063–1066.